Transportation Research Part B 147 (2021) 197–219

Contents lists available at ScienceDirect

Transportation Research Part B

journal homepage: www.elsevier.com/locate/trb

Optimal rebalancing and on-board charging of shared electric scooters

Jesus Osorio[a], Chao Lei[b], Yanfeng Ouyang[a,*]

[a] Department of Civil and Environmental Engineering, University of Illinois at Urbana-Champaign, Urbana, IL 61801, USA
[b] College of Transport and Communications, Shanghai Maritime University, Shanghai 201306, China

ARTICLE INFO

Article history:
Received 3 August 2020
Revised 30 December 2020
Accepted 22 March 2021
Available online 11 April 2021

Keywords:
Electric scooter
Sharing
Micromobility
Mixed-integer program
Continuous approximation

ABSTRACT

This paper presents a sequence of models for optimal overnight charging and rebalancing of shared electric scooters (e-scooters) by allowing e-scooters to be charged while being transported on rebalancing vehicles. This problem is first modeled as a mixed-integer program for the multi-commodity inventory routing problem, where commodities represent e-scooters with different states of charge. To avoid prohibitive computation burden, continuous approximation techniques are proposed to estimate costs associated with the pickup and drop-off operations in small local neighborhoods, and the formulation turns into a discrete-continuous hybrid model for the integrated operations at both local and line-haul levels. A series of numerical experiments are conducted to demonstrate that, as compared to direct application of the discrete formulation, the proposed hybrid approach can produce good quality solutions for large-scale instances in a much shorter computation time.

1. Introduction

Shared electric scooter (e-scooter) has recently become a popular mode of micromobility in the U.S. Since the first introduction in California in 2017, companies such as Bird, Lime and Jump have expanded their services to nearly 100 U.S. cities and deployed a total of over 85,000 e-scooters. According to the National Association of City Transportation Officials (NACTO), the total number of micromobility trips in the U.S. in 2019 (about 136 million) increased by about 62% as compared to that of the previous year (about 88.5 million), primarily due to the 50 million new trips by shared e-scooters in that year (National Association of City Transportation Officials, 2018; 2019).

However, such a rapid growth of e-scooter sharing services also causes significant operational challenges. E-scooter sharing companies must manage a total fleet size of over 10,000 e-scooters in large cities such as Los Angeles, San Francisco, and Austin, and those e-scooters would inevitably require overnight charging and repositioning (or rebalancing) over space so as to better capture the demand in the next day. Currently, one prevailing way to conduct these operations is that companies pay individual contractors to perform overnight charging and placement of e-scooters at certain locations. For such a "crowd charging" approach to work, companies usually need to pay around $4 to $5 per e-scooter per night depending on the e-scooters location and battery level (Elkins, 2019; Domonoske, 2019), as compared to only between $0.10 and $0.40 electricity cost to charge one e-scooter to full battery, according to *Bird* (Ha, 2019). Taking into account the fact that an e-scooter generates about $13 in revenue per day on average (Griswold, 2019), companies are spending a significant amount of their

* Corresponding author.
E-mail address: yfouyang@illinois.edu (Y. Ouyang).

https://doi.org/10.1016/j.trb.2021.03.009
0191-2615/

gross revenue on handling, charging and repositioning operations (Team, 2018). As such, the outsourcing cost for engaging contractors is rather high and there is a considerable margin to save charging cost. In addition, the outsourcing approach cannot always guarantee a reliable service, since its performance would highly depend on the engagement and dedication of individual contractors. Consequently, how to get all e-scooters properly charged and rebalanced in a cost-effective way has become a major operational challenge for e-scooter sharing companies.

One potential solution to these challenges is that companies can perform their own overnight charging and rebalancing operations, such that they can consolidate both operations in a smart way and potentially take advantage of "economies of scale". Furthermore, recently emerging battery technologies such as portable and fast-charging capabilities (Toll, 2019; Buchmann, 2020; StoreDot, 2020; GBatteries, 2020) can allow e-scooters to be quickly charged while being shipped during rebalancing operations. It is easy to see that this strategy not only eliminates the need to pay for expensive independent contractors but also avoids moving e-scooters to/from charging stations solely for the purpose of charging. Additionally, by hiring trained employees (instead of independent contractors) to handle e-scooters, the lifespan of e-scooters can be potentially increased, and in turn, the operating costs can be significantly reduced in the long run. Nonetheless, implementing this strategy is non-trivial. The company must create a charging-and-routing plan which simultaneously takes into account the state of charge (SoC) of all on-board e-scooters while determining an efficient pickup and drop-off strategy. In the temporal dimension, the charging time of e-scooters (which are picked up along the route) must be long enough so that e-scooters can be sufficiently charged before being dropped off at the expected demand locations. Meanwhile, in the spatial dimension, the rebalancing vehicle routes must remain under a reasonable length limit so as to reduce cost and to complete the necessary operations before the upcoming morning.

This paper develops a systematic optimization approach to overcome the challenges that come with the joint decision on charging and rebalancing operations for e-scooter sharing systems. An e-scooter rebalancing and charging problem (ES-RCP) is formulated to consider the trade-offs between efficient routing and charging times, while remaining efficient when handling large-scale problems. We first present a discrete inventory routing problem formulation, which considers e-scooters of different SoC as separate commodities linked through a transition function based on the charging capabilities of the rebalancing vehicles. Then, we seek computational enhancement for large-scale instances by embedding a continuous approximation (CA) subroutine (which estimates costs for routing decisions in local areas) into the discrete formulation. A series of numerical experiments, including hypothetical problem instances and a full-scale case study, are conducted to demonstrate the applicability and effectiveness of the proposed hybrid approach for large-scale instances.

The remainder of the paper is organized as follows: Section 2 discusses the related literature, including that on shared bike rebalancing, one-way electric vehicle systems, and continuous approximation. Section 3 presents the mathematical modeling including both the discrete and hybrid models. Section 4 presents the numerical experiments. Section 5 presents the conclusion and discusses future research directions. A list of notation is presented in the appendix.

2. Literature review

Despite the rapid surge of e-scooter sharing in many cities, there is still a lack of literature on operator-based rebalancing and charging operations for e-scooter sharing services. Some very recent work only addressed some relevant aspects of the problem. For example, Pender et al. (2020) developed high-level stochastic models to understand battery life dynamics for e-scooters in a large network, and to determine the number of battery swappers (i.e., workers) needed to maintain a certain level of service. Another relevant study by Masoud et al. (2019) focused on the scooter-to-charger assignment problem which arises from the crowd-charging approach currently used by e-scooter companies. To the best of our knowledge, no effort has been made to systematically account for the battery state as well as the spatial distribution of the e-scooters.

The closest literature on rebalancing operations has been studying bike-sharing systems (BSS), and the problem is usually modeled as the discrete one-commodity pickup and delivery traveling salesman problem (1-TSPPD) or the vehicle routing problem (1-VRPPD) (Hernández-Pérez and Salazar-González, 2003; Parragh et al., 2008), in which vehicles are typically used to transport bikes from locations with excess supply to locations with deficit. Although numerous studies have proposed formulation and solution methodologies for static (Chemla et al., 2013; Raviv et al., 2013; Dell'Amico et al., 2014; Ho and Szeto, 2014; Erdoğan et al., 2015; Forma et al., 2015; Alvarez-Valdes et al., 2016; Schuijbroek et al., 2017; Lei and Ouyang, 2018; Ho and Szeto, 2017; Liu et al., 2018) or dynamic bike-sharing rebalancing problems (Caggiani and Ottomanelli, 2012; Kloimüllner et al., 2014; Brinkmann et al., 2015; Labadi et al., 2015; Raviv and Kolka, 2013; Regue and Recker, 2014; Sayarshad et al., 2012; Zhang et al., 2017), none of them considered the commodity's change of state (i.e., charging of e-scooters) during the rebalancing operations. First of all, the batteries of the e-scooter can be in a variety of states of charge (SoC), which introduces complexity because the rebalancing problem more closely resembles a multi-commodity vehicle routing problem (Hernández-Pérez and Salazar-González, 2014). Although rebalancing operations with multiple bike types has been considered before (Li et al., 2016), in the e-scooter version of the problem is even more complex because the different e-scooter types (i.e., with different SoC) are allowed to change states on board over time. Another main characteristic of the ES-RCP is the absence of fixed charging docks, since in current services, e-scooters are allowed to park anywhere within a service region resembling a dock-less bike-sharing system (DBSS). As a result, the problem size of ES-RCP is expected to be large because dockless e-scooters can be parked anywhere (Pal and Zhang, 2017). In the literature, most studies on the dockless bike rebalancing problem reduce the size of the problem against the spatial sparsity of the fleet by generating spatial clusters or zones. As such, instead of defining the operations by considering the movement of each individual bike,

the rebalancing operations are described by aggregated flow of bikes in between clusters (Reiss and Bogenberger, 2015; 2016; Caggiani et al., 2017; 2018; Liu and Xu, 2018; Barabonkov et al., 2020; Fan et al., 2020). In this work, the supply and demand of e-scooters are defined on discrete nodes which represent small spatial neighborhoods such as roadway intersections, building entrances, or transit stops (where parked e-scooters usually cluster).

Nonetheless, in the ES-RCP, knowing the distribution of demand nodes or even the flow of e-scooters between surplus and deficit areas is not enough, because the e-scooters must also be recharged. Therefore, information on the SoC of all e-scooter batteries must be known to integrate the vehicle rebalancing operations with the charging of e-scooters over time. To this end, joint consideration of charging and rebalancing operations has been studied for electric vehicles (EVs). These application contexts include BSS rebalancing operations performed with EVs as well as operations of one-way electric car-sharing systems. Usama et al. (2019) considered bike rebalancing operations with battery-powered EVs, which are only allowed to be charged at the depot (under a linear charging/discharging rate) through multiple depot visits. They noted that the battery capacity can have a significant effect on the routing plan of the vehicle. Regarding one-way electric car-sharing services, the relocation problem has similarities to the ES-RCP because EVs are moved and charged by hired workers among stations to meet the user demand (Illgen and Höck, 2019; Brandstätter et al., 2016). Yet, the charging of EVs is only possible at fixed locations (e.g., parking lots or stations) when the EVs are stationary. In such problems, the most common methodology to account for time-dependent service (due to charging operations) is to implement a spatiotemporal graph to account for the time when vehicles are unavailable to the user (Gambella et al., 2018; Ait-Ouahmed et al., 2018; Xu et al., 2018; Bruglieri et al., 2014). However, it is well known that spatiotemporal graphs grow exponentially in size with the discretization of time and drastically increase the complexity of the problem. Li et al. (2016) overcame this challenge by applying a continuous approximation model to develop a comprehensive design framework for one-way EV car-sharing systems, in which the studied area is partitioned into small neighborhoods to easily approximate non-linear vehicle charging times.

CA models have often been used as an efficient alternative approach for providing performance estimates for large-scale location and vehicle routing problems (Daganzo, 2005; Hall, 1985; Hajibabai and Ouyang, 2016; Lei et al., 2019; Max Shen and Qi, 2007); see Ansari et al. (2018) for a comprehensive review. Lei and Ouyang (2018) developed a discrete-continuous modeling approach for 1-VRPPD by splitting vehicle travels into line-haul and local tours and solving large scale problems with a Lagrangian relaxation approach. Other researchers have applied CA concepts to model vehicle sharing systems, which aimed to inform strategic decisions such as the number and overall size of docking stations, fleet size, rebalancing period length, and system performance for docked and dock-less bike-sharing systems (Daganzo and Ouyang, 2019; Soriguera and Jiménez-Meroño, 2020). This paper focuses on the operations of the ES-RCP; the CA approach is used to propose a discrete-continuous hybrid model at the operational level, as in Lei and Ouyang (2018), where well-known asymptotic approximations (Daganzo, 1984b; Beardwood et al., 1959) are applied to estimate the performance of local routing and service strategies. Similar treatments in the temporal dimension are also used to approximate the charging of the e-scooters at the local level for large scale ES-RCPs.

While appearing to be similar to the dockless bike sharing, e-scooter sharing is a relatively new mode of transportation that comes with its unique logistical challenges. These challenges arise not only because of the large fleet deployed in dense urban areas but also because the e-scooters must inevitably be charged. This additional consideration adds an extra dimension of complexity to the traditional management of micromobility systems. The relatively small size of the e-scooters makes it suitable for charging while on-board of the rebalancing vehicles, which opens up new opportunity for cost savings through exploration of simultaneous charging and rebalancing.[1] As such, the following section presents the mathematical models and solution approaches proposed to solve the ES-RCP.

3. Mathematical models

In this section, we first present the notation, key assumptions and a discrete mixed-integer program formulation for ES-RCP. Then, a hybrid modeling approach is introduced for large scale instances. Finally, a methodology to generate a feasible solution from the hybrid model solution is explained.

3.1. Discrete model

We assume that all e-scooters are distributed on a set of discrete nodes (small neighborhoods) in a network $G(\mathcal{N}, \mathcal{A})$, where $\mathcal{N}$ is the set of nodes and $\mathcal{A} = \{(i, j)|i, j \in \mathcal{N}, i \neq j\}$ is the set of arcs. For modeling convenience, we assume that all the e-scooters share the same battery characteristics, and can be categorized into a set of types, denoted by $\mathcal{B} = \{1, 2, \ldots, B\}$, according to their SoC. Type B represents sufficiently charged e-scooters ready for drop-off. For instance, Fig. 1a presents an example of SoC change as a function of time, where $B = 10$ and each battery level represents a 10% SoC increment[2]; e-

[1] The charging and rebalancing problem in this paper also applies to e-bikes, or other types of vehicle sharing services that require repositioning and maintenance in between service periods. However, e-scooters tend to have smaller sizes and weights that are most suitable for the type of operations studied in this paper. For companies such as Lime and Jump, the e-bikes have been recorded to weigh over 73 pounds (Swift, 2019), while Lime e-scooters are about 27 pounds (Toll, 2018). This, along with the smaller size of e-scooters, makes them more suitable for easy transportation, and handling.

[2] In general, however, battery levels do not necessarily have to be defined over fixed increments.

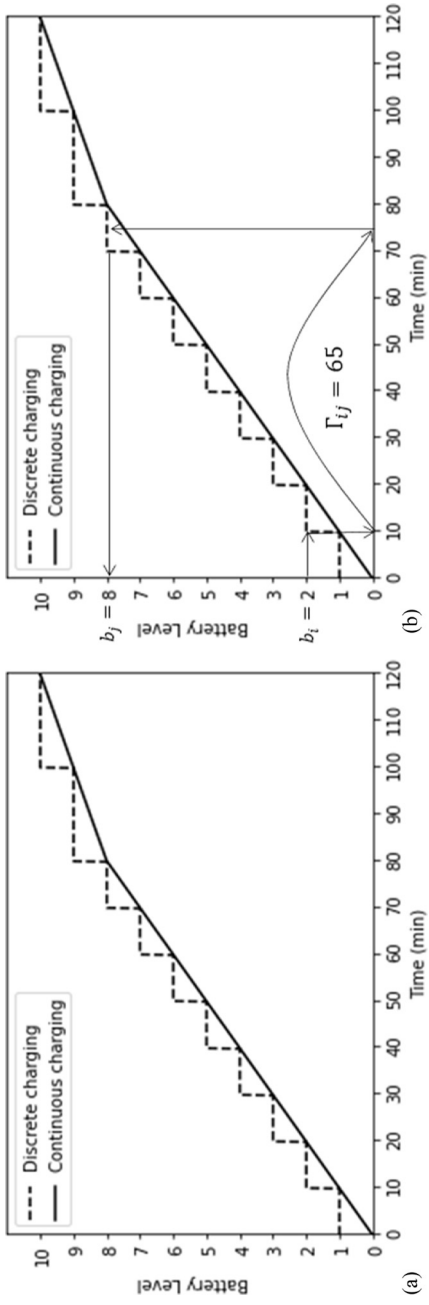

Fig. 1. (a) Example of charging function discretization into $B = 10$ levels. (b) Example of label updates from b_i to b_j according to the total travel time between nodes i and j, Γ_{ij}.

scooters with a SoC above 90% are considered "full" and ready for drop off. Each node $i \in \mathcal{N}$ is associated with a certain amount of pickup demand, i.e., the number of deficient types of e-scooters that are available to be picked up there, denoted by $P_{i,b}$ $\forall i \in \mathcal{N}, b \in \mathcal{B}$ and a certain amount of drop-off demand, i.e., the number of charged e-scooters that are desired at node i to meet a target level, denoted by D_i. Since the drop-off e-scooters should typically be sufficiently charged, here we simply assume that only the e-scooters with the highest battery SoC, B, can be dropped off. Hence, the index for the battery level is omitted in the drop-off demand notation, D_i. The operator is assumed to have information about the number of e-scooters needed to serve a given area in the following day, which is typically estimated through historical data or from a separate strategic planning model (Reiss and Bogenberger, 2016; Caggiani et al., 2017).

In this paper, we assume that a set of designated rebalancing vehicles with a carrying capacity Q, denoted by $\mathcal{V}$, are responsible for rebalancing and charging e-scooters over the network. That being so, each vehicle is assumed to operate at a constant speed s, and start and end their tours at the depots O and S, respectively. For convenience, we assume that all on-board e-scooter can be continuously charged as needed. Therefore, the charging capacity of trucks is not modeled, nor is it assumed to be a limiting factor for the length of vehicle tours.[3] Consequently, the decision maker can extend the charging time of on-board e-scooters by delaying the vehicles (e.g., enforcing a lower speed, introducing a detour, or dwelling at some locations). Such options are reflected by allowing vehicles to dwell at a subset of nodes, denoted by $\mathcal{M} \subset \mathcal{N}$, for a certain length of slack time. Then, each vehicle can be in three types of modes: (i) picking up or dropping off e-scooters at a node; (ii) moving from one node to another; and (iii) waiting at permissible nodes. The length of waiting time is assumed to take value from a set of discrete options, denoted by $\mathcal{L}_i$; e.g., $\mathcal{L}_i = \{0 \text{ min}, 5 \text{ min}, \ldots, 60 \text{ min}\}, \forall i \in \mathcal{M}$ and $\mathcal{L}_i = \{0 \text{ min}\}, \forall i \in \mathcal{N} \setminus \mathcal{M}$. As such, the routing and waiting decisions of the vehicles can be integrated into a single set of binary variables, $\{x_{v,i,j,l}\}$; i.e., $x_{v,i,j,l} = 1$ if vehicle $v \in \mathcal{V}$ travels through arc $(i, j) \in \mathcal{A}$ after waiting $l \in \mathcal{L}_i$ length of time at node $i \in \mathcal{N}$, or 0 otherwise. The charging duration from node i to j, denoted by Γ_{ij}, can be calculated as the summation of the pickup/drop-off duration τ,[4] the waiting time at node i, l_i, and the travel time on arc t_{ij}; i.e.,

$$\Gamma_{ij} = \tau + l_i + t_{ij}, \forall (i, j) \in \mathcal{A}. \tag{1}$$

In order to keep track of the tour times of the vehicles, another set of variables $\{u_{v,i}\}$ are defined to track the arrival time of vehicles at nodes; $u_{v,j} = u_{v,i} + \Gamma_{i,j}$ if vehicle i spends $\Gamma_{i,j}$ time to travel to node j.

The on-board e-scooters can change state between two consecutive stops as the result of two factors: the initial state of e-scooters and the charging duration. In practice, e-scooters are typically powered by lithium-ion batteries, which means the charging curve is likely to be roughly piecewise linear with a threshold at SoC $\approx$ 80%, as shown in Fig. 1a (Montoya et al., 2017). We propose a general state transition function, f, which maps the battery level of type b e-scooters at node i, denoted by b_i, and the charging duration Γ_{ij}, to the type e-scooters upon arriving at node j, denoted by b_j. For instance, in the example shown in Fig. 1b, $b_j = f(b_i = 2, \Gamma_{ij} = 65 \text{ min}) = 8$. Because of the nonlinearity of the charging function, the transition function f does not necessarily produce a one-to-one mapping, i.e., it is possible that e-scooters with distinct battery levels at node i transform into those with an identical battery level at node j. One simple and intuitive example is that if a vehicle waits long enough at a node i, all e-scooters on board would become type B e-scooters. Therefore, we define a set $\mathcal{C}_{b,i,j,l}$ to store all e-scooter types that would transition to type $b \in \mathcal{B}$ after a vehicle waits $l \in \mathcal{L}_i$ units of time at node $i \in \mathcal{N}$ and traverses to node $j \in \mathcal{N}$. In the example of Fig. 1b, $\mathcal{C}_{8,i,j,l} = \{2\}$ because type 2 e-scooters will become type 8 e-scooters. In case that no initial battery levels can be mapped to a battery level b, then $\mathcal{C}_{b,i,j,l} = \emptyset$. This case typically arises when the arc is very long, as in Fig. 1b (i.e., all e-scooters are charged to higher battery levels).

Now we can keep track of the inventory of on-board e-scooters along the tour. Let $q_{v,i,b}$ denote the number of type $b \in \mathcal{B}$ e-scooters on vehicle $v \in \mathcal{V}$ when arriving at node $i \in \mathcal{N}$. Furthermore, let $\theta^+_{v,i,b}$ and $\theta^-_{v,i}$ be the numbers of type $b \in \mathcal{B}$ e-scooters to be picked up and dropped off by vehicle $v \in \mathcal{V}$ at node $i \in \mathcal{N}$, respectively. After traversing arc (i, j), i.e., $x_{v,i,j,l} = 1$, it can be updated as follows:

$$q_{v,j,b} = \begin{cases} \sum_{b' \in \mathcal{C}_{b,i,j,l}} \left(q_{v,i,b'} + \theta^+_{v,i,b'} \right) - \theta^-_{v,i}, & \text{if } b = B, \\ \sum_{b' \in \mathcal{C}_{B,i,j,l}} \left(q_{v,i,b'} + \theta^+_{v,i,b'} \right), & \text{otherwise} \end{cases}, \forall b \in \mathcal{B}, v \in \mathcal{V}, (i, j) \in \mathcal{A}. \tag{2}$$

Eq. (2) updates the label of the e-scooters on board as the vehicle moves through the network; it does not allow drop-offs of e-scooters with $b < B$, and hence only includes drop-off decision variable $\theta^-_{v,i}$ when $b = B$. It is important to mention that there is an approximation error due to the discretization of the SoC, making the charging quantity tracked by the discrete model a conservative estimate of the real value. For instance, in Fig. 1b, even when the transition function landed halfway between battery levels 8 and 9, the partial charging between those battery levels is lost the moment the truck travels from node j to another node. This error however is found in our numerical experiments to be negligible for most reasonable values of B.

[3] We understand that the charging rates and charging capacity may be of concern in practice, but this could be achieved with emerging ultra-fast and fast charging technologies which can charge the e-scooters within minutes. Moreover, portable generators can be used in trucks in order to achieve the high voltage needed for faster charging.

[4] In reality, the e-scooters picked up at a node would only charge for $t_{ij} + l_i$, but for simplicity, we assume all e-scooters, including the ones picked up at a node i, experience a charging time of $\tau + l_i + t_{ij}$.

The primary objective of the company is to maximize the potential benefits for fulfilling the demand while minimizing the total operational costs. The operational costs mainly consist of three components: the fixed cost of deploying vehicles (i.e., including cost for drivers/staff), the travel cost, and the extra penalty for having a non-zero on-board e-scooter inventory for distribution at the beginning of the tours. It is assumed that the operator has fully-charged backup e-scooters at the depot that help vehicles do "start-up operations (i.e., drop-offs) at the beginning of the operation period. These backup e-scooters would not be in service during the day, which is why there is a penalty for the used backup e-scooters.

Denoting c_{veh} as the fixed cost for deploying a rebalancing vehicle in units of cost per vehicle deployment, c_{dist} as the cost per unit distance traveled by a rebalancing vehicle, c_{extra} as the non-zero initial inventory penalty per e-scooter, the total operational cost, denoted by TC, can be formulated as

$$TC = c_{\text{veh}} \sum_{v\in\mathcal{V}} \sum_{j\in\mathcal{N}} x_{v,O,j,0} + c_{\text{dist}} \sum_{v\in\mathcal{V}} \sum_{i\in\mathcal{N}\cup O} \sum_{j\in\mathcal{N}\cup S} \sum_{l\in\mathcal{L}_i} d_{ij} x_{v,i,j,l} + c_{\text{extra}} \sum_{v\in\mathcal{V}} \sum_{b\in\mathcal{B}} q_{v,O,b}. \tag{3}$$

On the other hand, the benefit from the rebalancing and charging operations includes two parts: that from fulfilling the drop-off demand, and that for clearing deficient e-scooters from the system. The revenue produced by dropping off an e-scooter, c_{drop}, is assumed be positive only for type B e-scooters. The monetary benefit for picking a type b e-scooter, denoted by $c_{\text{pick},b}$, can be interpreted as the benefit associated with the "convenience" of the users for removing non-functioning e-scooters on sidewalks. Therefore, $c_{\text{pick},b}$ is the highest for $b = 1$ and decreases for higher battery levels. The total benefit can be written as

$$TB = \sum_{v\in\mathcal{V}} \sum_{i\in\mathcal{N}} c_{\text{drop}} \theta^-_{v,i} + \sum_{v\in\mathcal{V}} \sum_{i\in\mathcal{N}} \sum_{b\in\mathcal{B}} c_{\text{pick},b} \theta^+_{v,i,b}. \tag{4}$$

At this point, the discrete mathematical formulation of the e-scooter rebalancing and charging problem can be presented as follows:

$$\max \quad TB - TC \tag{5}$$

s.t.(14), (15), (16), (17),

$$\sum_{j\in\mathcal{N}\cup S} \sum_{l\in\mathcal{L}_i} x_{v,i,j,l} = \sum_{j\in\mathcal{N}\cup O} \sum_{l\in\mathcal{L}_j} x_{v,j,i,l} \le 1, \quad \forall v \in \mathcal{V}, i \in \mathcal{N} \tag{6}$$

$$\sum_{v\in\mathcal{V}} \sum_{i\in\mathcal{N}\cup O} \sum_{l\in\mathcal{L}_i} x_{v,i,j,l} \le 1, \quad \forall j \in \mathcal{N} \tag{7}$$

$$\theta^+_{v,i,b} \le P_{i,b} \sum_{j\in\mathcal{N}\cup S} \sum_{l\in\mathcal{L}_i} x_{v,i,j,l}, \quad \forall v \in \mathcal{V}, i \in \mathcal{N}\cup O, b \in \mathcal{B} \tag{8}$$

$$\theta^-_{v,i} \le D_i \sum_{j\in\mathcal{N}\cup S} \sum_{l\in\mathcal{L}_i} x_{v,i,j,l}, \quad \forall v \in \mathcal{V}, i \in \mathcal{N}\cup O \tag{9}$$

$$u_{v,i} + \Gamma_{ij} \le u_{v,j} + M(1 - x_{v,i,j,l}), \quad \forall v \in \mathcal{V}, (i,j) \in \mathcal{A}, l \in \mathcal{L}_i \tag{10}$$

$$u_{v,i} + \Gamma_{ij} \ge u_{v,j} - M(1 - x_{v,i,j,l}), \quad \forall v \in \mathcal{V}, (i,j) \in \mathcal{A}, l \in \mathcal{L}_i \tag{11}$$

$$u_{v,O} = 0, \quad \forall v \in \mathcal{V} \tag{12}$$

$$u_{v,S} \le T, \quad \forall v \in \mathcal{V} \tag{13}$$

$$q_{v,j,b} \ge \sum_{b'\in\mathcal{C}_{b,i,j,l}} \left(q_{v,i,b'} + \theta^+_{v,i,b'}\right) - M(1 - x_{v,i,j,l}), \quad \forall v \in \mathcal{V}, (i,j) \in \mathcal{A}, b \in \mathcal{B}\setminus\{B\}, l \in \mathcal{L}_i, \tag{14}$$

$$q_{v,j,b} \le \sum_{b'\in\mathcal{C}_{b,i,j,l}} \left(q_{v,i,b'} + \theta^+_{v,i,b'}\right) + M(1 - x_{v,i,j,l}), \quad \forall v \in \mathcal{V}, (i,j) \in \mathcal{A}, b \in \mathcal{B}\setminus\{B\}, l \in \mathcal{L}_i, \tag{15}$$

$$q_{v,j,B} \ge \sum_{b'\in\mathcal{C}_{B,i,j,l}} \left(q_{v,i,b'} + \theta^+_{v,i,b'}\right) - \theta^-_{v,i} - M(1 - x_{v,i,j,l}), \quad \forall v \in \mathcal{V}, (i,j) \in \mathcal{A}, l \in \mathcal{L}_i, \tag{16}$$

$$q_{v,j,B} \le \sum_{b'\in\mathcal{C}_{B,i,j,l}} \left(q_{v,i,b'} + \theta^+_{v,i,b'}\right) - \theta^-_{v,i} + M(1 - x_{v,i,j,l}), \quad \forall v \in \mathcal{V}, (i,j) \in \mathcal{A}, l \in \mathcal{L}_i. \tag{17}$$

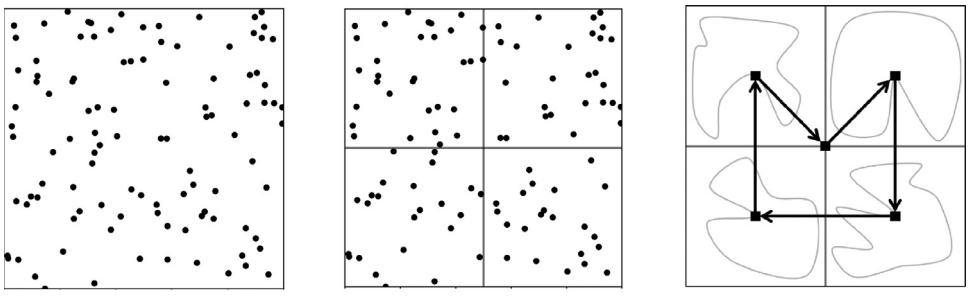

Fig. 2. CA-based hybrid modeling framework; (a) discrete demand nodes; (b) partition of homogeneous regions; (c) routing plan including local service and line-haul trips between zones.

$$\sum_{b\in\mathcal{B}} q_{v,i,b} \le Q \sum_{j\in N\cup S}\sum_{l\in\mathcal{L}_i} x_{v,i,j,l}, \quad \forall v\in\mathcal{V}, i\in\mathcal{N}\cup O \tag{18}$$

$$q_{v,i,B} \ge \theta^{-}_{v,i}, \quad \forall v\in\mathcal{V}, i\in\mathcal{N}\cup O\cup S \tag{19}$$

$$x_{v,i,j,l}\in\{0,1\}, \quad \forall v\in\mathcal{V}, (i,j)\in\mathcal{A}, l\in\mathcal{L}_i \tag{20}$$

$$\theta^{+}_{v,i,b}, \theta^{-}_{v,i}, q_{v,i,b} \ge 0, \quad \forall v\in\mathcal{V}, i\in\mathcal{N}\cup O\cup S, b\in\mathcal{B} \tag{21}$$

$$u_{v,i}\ge 0, \quad \forall v\in\mathcal{V}, i\in\mathcal{N}\cup O\cup S \tag{22}$$

The objective function (5) maximizes the expected revenues minus the total cost. Constraints (6) and (7) enforce conservation of vehicles, and that each node can be visited at most once. Constraints (8) and (9) enforce the demand constraints. Constraints (10)–(13) present the time constraints per vehicle. Constraints (14)–(17) are linearized versions of Eq. (2), utilizing a big number M (which could be set as the largest possible value of the $\{q_{v,i,b}\}$ variables). They update the inventory of e-scooters on the vehicles according to the routing and waiting decisions (e.g., when the corresponding $x_{v,i,j,l}$ variable equals 1). Constraints (18) enforce the capacity of the vehicle, while constraints (19) indicate that one cannot drop off more e-scooters than the number on board. Finally, constraints (20)–(22) define binary and nonnegative variables.

The above mixed-integer program is challenging to solve due to multiple vehicles, large number of nodes, and large number of battery levels. In particular, if B is large, the discrete charging function better approximates the continuous charging curve, but this results in a large set $\mathcal{B}$, which in turn increases the number of constraints, the number of transition in the set $\mathcal{C}_{b,i,j,l}$, and hence the computational difficulty of the problem. On the other hand, if B is too small, the effectiveness of onboard charging will be largely inaccurate. The choice of B should clearly depend on the link travel times in the network and the battery charging rate; e.g., a sparse network containing only long arcs and a fast charging rate could allow smaller B. Technically, one should pick B such that the time to charge e-scooters from b to $b+1$ is comparable to $\min\{t_{ij}: \forall (i,j)\in\mathcal{A}\}$.

3.2. Hybrid model

To address the aforementioned computational challenges, we propose a discrete and continuous hybrid approach to the e-scooter rebalancing and charging problem. The basic idea is to approximately consolidate the detailed operational decisions at the nodes in a local neighborhood (called as "zone" from now on) into only a few decision variables, and model the complementing inter-zonal operations over a much smaller size network (now with zones replacing the nodes) through the discrete modeling approach.

We assume that the entire service area containing discrete demand nodes can be partitioned into a set of disjoint zones $\mathcal{Z}=\{1,2,\ldots,|\mathcal{Z}|\}$ (see Fig. 2a and b), where the nodes in each zone are uniformly distributed and the associated pickup/drop-off demand is approximately homogeneous.[5] We also assume that the distribution of nodes is so dense that

[5] In practice, we understand that this may be challenging to achieve since the homogeneity of zones is defined regarding the spatial distribution of nodes and the SoC of e-scooters. Zone partitioning is a step performed in the data processing stage, possibly through hierarchical clustering methods, and is assumed to be given as an input. Our experience tells us that the CA models are robust even when homogeneity is not strictly satisfied (Daganzo, 2005). Furthermore, the modeler could select both the number of battery levels and the SoC ranges for each battery level in order to maximize the homogeneity within the zones.

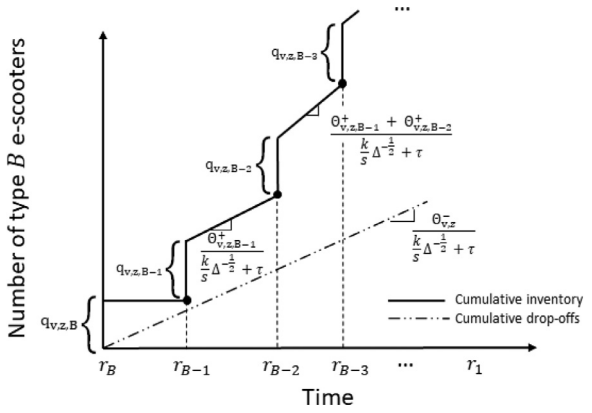

Fig. 3. Cumulative inventory of type B e-scooters when vehicles perform the local service.

the number of nodes within each zone is still large. In this way, we can use the average number of type $b \in \mathcal{B}$ e-scooters per node, denoted by $\bar{P}_{z,b}$, and the average number of e-scooters to be dropped off per node, denoted by $\bar{D}_z$, to represent the pickup and drop-off demand in zone $z \in \mathcal{Z}$, respectively. The operator's decisions then become determining a routing plan for the zones to be visited as well as constructing a local operation strategy (i.e., picking up and dropping off different types of e-scooters) within each zone. As such, the entire routing plan of a vehicle can be decomposed into two types: (i) the local tours within each visited zone to fulfill the pickup and drop-off demand at each individual node, and (ii) the line-haul trips across different zones. The modeling frameworks for each type of trips are presented in the following sections.

3.2.1. Local approximation

Let a_z denote the area of zone $z \in \mathcal{Z}$ and Δ_z as the node density. When the number of nodes in zone $z \in \mathcal{Z}$ is sufficiently large, i.e., $a_z \Delta_z \gg 1$, and when the nodes within a zone share homogeneous demand characteristics, we perform an identical service strategy for all the nodes, i.e., picking up and/or dropping off the same number of e-scooters of each type, such that the zone can still remain homogeneous after the rebalancing operation. Here we simply assume that a vehicle would follow the optimal TSP tour to visit all the nodes within a zone. According to Beardwood et al. (1959); Daganzo (2005), the length that each stop in the TSP tour contributes toward the total traveling distance in zone z is asymptotically comparable with the average separation between neighboring points, i.e., $k(\Delta_z)^{-\frac{1}{2}}$, where k is a dimensionless parameter that depends on the distance metric only. We can then estimate the total travel time within a zone as follows:

$$\Pi_z = \frac{1}{s} k(\Delta_z)^{\frac{1}{2}} a_z + \tau \Delta_z a_z, \forall z \in \mathcal{Z}, \tag{23}$$

where the two terms on the right-hand side represent the estimated total motion time and the total stopping time for performing pickup/drop-off operations in zone $z \in \mathcal{Z}$, respectively.

Following the TSP touring plan and the identical pickup and drop-off strategy, the planner only needs to determine two kinds of decisions to characterize how a zone z would be served, i.e., (i) the average number of sufficiently charged e-scooters to be dropped off at each node by vehicle v, denoted by $\Theta^-_{v,z}$, and (ii) the average number of type b e-scooters to be picked up at each node by vehicle v, denoted by $\Theta^+_{v,z,b}$. Note that these decisions must satisfy the load and charging constraints so as to guarantee a feasible operational plan, and the most critical issue for fulfilling this task is to keep track of the amount of on-board e-scooters by type along the tour. To define the load and transition constraints, we use the two variables $q_{v,z,b}$ and $q'_{v,z,b}$ denote the type b e-scooters on-board before and after the local tour, respectively. We need to guarantee that the load level stays under the capacity limit Q, and meanwhile, there are enough sufficiently charged type B e-scooters to be dropped off at each node.

First we look into the inventory level of type B e-scooters along the tour. In Fig. 3, we illustrate the cumulative inventory of type B e-scooters by the solid piece-wise linear curve and the cumulative drop-offs by a dash-dotted linear curve, where r_b denotes the amount of time needed to charge a type b e-scooter to a type B one (which can be computed from function f). The vertical jumps on the solid line captures the transition of the initially onboard type b e-scooters, $q_{v,z,b}$, to type B. Since $\Theta^+_{v,i,b}$, additional type b e-scooters will be picked up per $\frac{k}{s}(\Delta_z)^{-\frac{1}{2}} + \tau$ time along the tour, they would gradually become available for drop-off at an estimated rate of $\frac{\Theta^+_{v,i,b}}{\frac{k}{s}(\Delta_z)^{-\frac{1}{2}}+\tau}$, starting from time r_b. As such, the overall rate that e-scooters become available for drop-off between time r_{b+1} and r_b can be computed as

$$\sum_{b'=b+1}^{B} \frac{\Theta^+_{v,z,b'}}{\frac{k}{s}(\Delta_z)^{-\frac{1}{2}}+\tau}. \tag{24}$$

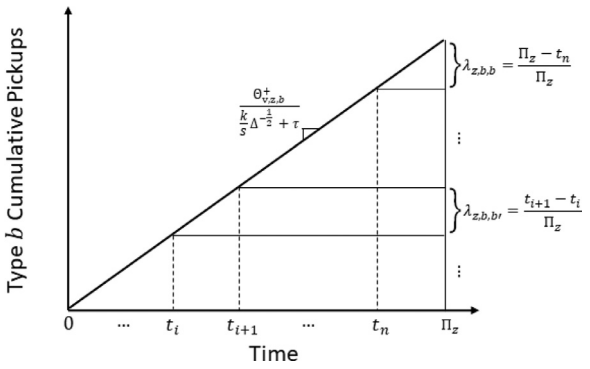

Fig. 4. Continuous local charging approximation the vehicle performs type b pickups.

Similarly, the drop-off curve has a constant slope of $\frac{\Theta^-_{v,z}}{\frac{k}{s}(\Delta_z)^{-\frac{1}{2}}+\tau}$.

The inventory level of type B e-scooters at an arbitrary time instant is the difference between the cumulative inventory curve and the cumulative drop-off curve. To ensure that there are enough type B e-scooters for drop-off, the drop-off curve cannot go above the cumulative inventory curve – to guarantee that, we only need to check those critical time instants at $r_b, \forall b \in \mathcal{B}$ (illustrated as black dots in Fig. 3).

Simple geometry shows that the sought condition is satisfied as long as:

$$\Theta^-_{v,z}\frac{r_b}{\frac{k}{s}(\Delta_z)^{-\frac{1}{2}}+\tau} \le \sum_{b'=b+1}^{B}\left(q_{v,z,b'} + \Theta^+_{v,z,b'}\frac{r_b - r_{b'}}{\frac{k}{s}(\Delta_z)^{-\frac{1}{2}}+\tau}\right),\ \forall v \in \mathcal{V}, z \in \mathcal{Z}, b \in \mathcal{B}\setminus\{B\} \text{ if } r_b \le \Pi_z. \tag{25}$$

The two sides of the above inequality compute the cumulative drop-off number and cumulative inventory value at every step r_b. Note that Eq. (25) only needs to be enforced for drop-offs up to the end of the tour; i.e., when $r_b \le \Pi_z$.

For all other battery levels $b < B$, no drop-offs are expected so we only need to track the initial inventory and the pickups along the tour (since battery transitions are "internal"). Given piece-wise linearity and constant slopes, we only need to ensure that $\sum_b q'_{v,z,b} \le Q$ and $\sum_b q_{v,z,b} \le Q\ \ \forall v \in V, z \in Z$ in order to meet the vehicle capacity constraints. For any zone $z \in \mathcal{Z}$, the value of Π_z is fixed, and the state transition of e-scooters within each zone is actually known and can be pre-processed. For example, for the initial e-scooter inventory, a similar $\mathcal{C}'_{z,b}$ table can be created to store all battery levels which can be charged up to battery level $b \in \mathcal{B}$ after serving zone z. For those e-scooters picked up en-route, some may be charged fully, while others may not experience any state transition. Fig. 4 illustrates the cumulative pickups and conversion of type b e-scooters along the tour. The set of time instants $\{t_i\}$ are defined from the transition function f, such that the duration from t_i to Π_z is the necessary charging time for a type b e-scooter to become a type $b' \ge b$ at the end of the tour. Then, parameter $\lambda_{z,b,b'}$ is the proportion of all e-scooters picked up in zone z from battery level b which are charged up to battery level b', as computed in Fig. 4. Similar calculation can be done for every battery level b for which $\Theta^+_{v,z,b} > 0$ in each zone. A set of transition constraints, as counterparts of (14)–(17), are applied; i.e., $\forall v \in \mathcal{V}, z \in \mathcal{Z}\cup O, z' \in \mathcal{Z}\cup S, b \in \mathcal{B}\setminus\{B\}, l \in \mathcal{L}_z$:

$$q'_{v,z,b} \ge \sum_{b' \in \mathcal{C}'_{z,b}}\left(q_{v,z,b'} + \Theta^+_{v,z,b'}a_z\Delta_z\lambda_{z,b',b}\right) - M(1 - x_{v,z,z',l}), \tag{26}$$

$$q'_{v,z,b} \le \sum_{b' \in \mathcal{C}'_{z,b}}\left(q_{v,z,b'} + \Theta^+_{v,z,b'}a_z\Delta_z\lambda_{z,b',b}\right) + M(1 - x_{v,z,z',l}), \tag{27}$$

$$q'_{v,z,B} \ge \sum_{b' \in \mathcal{C}'_{z,B}}\left(q_{v,z,b'} + \Theta^+_{v,z,b'}a_z\Delta_z\lambda_{z,b',B}\right) - \Theta^-_{v,z}a_z\Delta_z - M(1 - x_{v,z,z',l}), \tag{28}$$

$$q'_{v,z,B} \le \sum_{b' \in \mathcal{C}'_{z,B}}\left(q_{v,z,b'} + \Theta^+_{v,z,b'}a_z\Delta_z\lambda_{z,b',B}\right) - \Theta^-_{v,z}a_z\Delta_z + M(1 - x_{v,z,z',l}). \tag{29}$$

Once the onboard inventory at the end of the current local tour is obtained, it is used to generate the initial inventory at the beginning of the next zone. This calculation involves the decisions made at the line-haul level, and is presented in the following section.

3.2.2. Line-haul operations

At the line-haul level, the company needs to determine the routing and charging plan across zones, as shown in Fig. 2c. The line-haul trips can be modeled similarly as the discrete mathematical model by replacing the node set $\mathcal{N}$ with the zone

set $\mathcal{Z}$. Then, the decision variable $x_{v,z,z',l}$ in this context is interpreted as the decision of whether vehicle v serves zone z' after serving zone z, and waits $l \in \mathcal{L}_z$ units of time. Each line-haul trip is assumed to happen between zone centroids and the waiting is assumed to happen at z after the vehicle serves the zone. Similar to the discrete model, we can define a set $\mathcal{C}_{b,z,z',l}$ to store all the types of e-scooters that can transition to type b after traversing zone pair (z, z') and waiting l units of time. The total cost, TC, and the total benefit, TB, in the objective function can thus be formulated by using both the line-haul and local decision variables as follows:

$$TC = c_{\text{veh}} \sum_{v\in\mathcal{V}} \sum_{z\in\mathcal{Z}} x_{v,O,z,0} + c_{\text{extra}} \sum_{v\in\mathcal{V}} q'_{v,0,B} + c_{\text{dist}} \sum_{v\in\mathcal{V}} \sum_{z\in\mathcal{Z}\cup O} \sum_{z'\in\mathcal{Z}\cup S} \sum_{l\in\mathcal{L}_z} d_{z,z'} x_{v,z,z',l}, \tag{30}$$

$$TB = c_{\text{drop}} \sum_{v\in\mathcal{V}} \sum_{z\in\mathcal{Z}} \Theta^{-}_{v,z} a_z \Delta_z + \sum_{v\in\mathcal{V}} \sum_{z\in\mathcal{Z}} \sum_{b\in\mathcal{B}} c_{\text{pick},b} \Theta^{+}_{v,z,b} a_z \Delta_z. \tag{31}$$

By combining the line-haul and local models together, the integrated formulation is presented as follows:

$$\max \quad TB - TC \tag{32}$$

s.t. (25)-(31), and

$$\sum_{z'\in\mathcal{Z}\cup S} \sum_{l\in\mathcal{L}_z} x_{v,z,z',l} = \sum_{z'\in\mathcal{Z}\cup O} \sum_{l\in\mathcal{L}'_z} x_{v,z',z,l} \le 1, \quad \forall v \in \mathcal{V}, z \in \mathcal{Z}\cup O\cup S \tag{33}$$

$$\sum_{v\in\mathcal{V}} \sum_{z\in\mathcal{Z}\cup O} \sum_{l\in\mathcal{L}_z} x_{v,z,z',l} \le 1, \quad \forall z' \in \mathcal{Z} \tag{34}$$

$$\Theta^{+}_{v,z,b} \le \bar{P}_{z,b} \sum_{z'\in\mathcal{Z}\cup S} \sum_{l\in\mathcal{L}_z} x_{v,z,z',l}, \quad \forall v \in \mathcal{V}, z \in \mathcal{Z}\cup O, b \in \mathcal{B} \tag{35}$$

$$\Theta^{-}_{v,z} \le \bar{D}_z \sum_{z'\in\mathcal{Z}\cup S} \sum_{l\in\mathcal{L}_z} x_{v,z,z',l}, \quad \forall v \in \mathcal{V}, z \in \mathcal{Z}\cup O \tag{36}$$

$$u_{v,z} + \Pi_z + t_{zz'} + l \le u_{v,z'} + M(1 - x_{v,z,z',l}), \quad \forall v \in \mathcal{V}, z \in \mathcal{Z}\cup O, z' \in \mathcal{Z}\cup S, l \in \mathcal{L}_z \tag{37}$$

$$u_{v,z} + \Pi_z + t_{zz'} + l \ge u_{v,z'} - M(1 - x_{v,z,z',l}), \quad \forall v \in \mathcal{V}, z \in \mathcal{Z}\cup O, z' \in \mathcal{Z}\cup S, l \in \mathcal{L}_z \tag{38}$$

$$u_{v,O} = 0, \quad \forall v \in \mathcal{V} \tag{39}$$

$$u_{v,S} \le T, \quad \forall v \in \mathcal{V} \tag{40}$$

$$q_{v,z',b} \ge \sum_{b'\in\mathcal{C}_{b,z,z',l}} q'_{v,z,b'} - M(1 - x_{v,z,z',l}), \quad \forall v \in \mathcal{V}, z \in \mathcal{Z}\cup O, z' \in \mathcal{Z}\cup S, b \in \mathcal{B}, l \in \mathcal{L}_z \tag{41}$$

$$q_{v,z',b} \le \sum_{b'\in\mathcal{C}_{b,z,z',l}} q'_{v,z,b'} + M(1 - x_{v,z,z',l}), \quad \forall v \in \mathcal{V}, z \in \mathcal{Z}\cup O, z' \in \mathcal{Z}\cup S, b \in \mathcal{B}, l \in \mathcal{L}_z \tag{42}$$

$$\sum_{b\in\mathcal{B}} q_{v,z,b} \le Q \sum_{z'\in\mathcal{Z}\cup S} \sum_{l\in\mathcal{L}_z} x_{v,z,z',l}, \quad \forall v \in \mathcal{V}, z \in \mathcal{Z}\cup O \tag{43}$$

$$\sum_{b\in\mathcal{B}} q'_{v,z,b} \le Q \sum_{z'\in\mathcal{Z}\cup S} \sum_{l\in\mathcal{L}_z} x_{v,z,z',l}, \quad \forall v \in \mathcal{V}, z \in \mathcal{Z}\cup O \tag{44}$$

$$x_{v,z,z',l}, \in \{0, 1\}, \quad \forall v \in \mathcal{V}, z \in \mathcal{Z}\cup O, z' \in \mathcal{Z}\cup S, l \in \mathcal{L}_z \tag{45}$$

$$u_{v,z}, q_{v,z,b}, q'_{v,z,b} \Theta^{+}_{v,z,b}, \Theta^{-}_{v,z} \ge 0, \quad \forall v \in \mathcal{V}, z \in \mathcal{Z}\cup O\cup S, b \in \mathcal{B} \tag{46}$$

The objective function (32) is similar to the objective function (5) except now the distance is defined as the distance between zone centroids. Constraint (25) ensures there are enough e-scooters on board for drop-off along the local tour. Constraints (26)–(29) update the inventory based on the local tours according to the set $C'_{b,z}$ and parameter $\lambda_{z,b,b'}$. All other constraints, (33)–(44), are counterparts of constraints (6)–(18) from the discrete model which enforce the conservation of

vehicles, demand constraints, time constraints, battery transition constraints in line-haul trips, and capacity constraints. Finally, constraints (45) and (46) define binary and nonnegative variables.

Since $|\mathcal{Z}| \ll |\mathcal{N}|$, the time needed to solve this problem is much shorter than that needed for the original discrete model. This allows us to even solve the hybrid model with a greater number of battery levels. Nonetheless, the solution of the hybrid modeling approach only provides an approximation to the original problem. In practice, operators would still need to develop an implementable routing plan in the network. The following section describes how the output from the hybrid network approach can be turned into a feasible solution.

3.2.3. Generating a feasible solution

The output of the hybrid model includes the sequence of zones for each vehicle to visit, the total waiting at each zone, the initial inventory, and the average pickups and drop-offs for each e-scooter type in each zone. We next utilize this information to route the vehicle in the original network while enforcing all the inventory and charging constraints. The basic idea is to decouple the problem and first solve the routing of the vehicles, and then implement a simple heuristic to determine which e-scooters are picked up or dropped off along the routes.

We solve a TSP among the nodes within each zone and connect the zones in the sequence with the following simple rules:

- If there is a nonzero wait time $l > 0$ between zones z and z', the vehicle is assumed to wait at the centroid in zone z. Therefore, the vehicle is routed through zone z, and the destination node in the TSP solution of the local tour is set to be at the centroid of z. Then, the vehicle travels from the centroid of z to the nearest node $j \in z'$.
- If there is no wait between zones z and z', the TSP is routed through zone z and the destination node is set to the nearest node $j \in z'$ (i.e., no visits to the depot).

The TSP solution within each zone can be computed with most commercial solvers in reasonable computational times. However, if necessary, heuristics such as those in Daganzo (1984b,a); Newell and Daganzo (1986b,a); Ouyang (2007) can be applied to obtain feasible solutions. If it is found that a feasible vehicle routing time, including the waiting at the centroids, is greater than T, time is subtracted from the waiting times at each of the centroids until the tour time becomes feasible.

Once the feasible routing of the vehicle is obtained, two heuristics are proposed to generate a feasible solution. The first heuristic (from now on referred to as "CA heuristic 1") is to feed the routing of the vehicle, the waiting at centroids, and initial inventory from the CA model back into the discrete model, so the discrete model has to only make the pickup and drop-off decisions. This can be achieved by simply adding more constraints to the discrete model enforcing $x_{v,i,j,l} = 1$ for each traversed arc (i, j) in the TSP solution.

If the size of the problem is so large that CA heuristic 1 is still time-consuming, another simple heuristic can be applied to generate a feasible solution in a short amount of time. For this second heuristic (for now on referred to as "CA heuristic 2"), we know that for a zone z, the pickup and drop-off strategy is given by performing an average of $\Theta^{+}_{v,z,b}$ pickups and $\Theta^{-}_{v,z}$ drop-offs respectively. If in some specific node in a zone $P_{i,b} < \Theta^{+}_{v,z,b}$, then the operator is only limited to pick up $P_{i,b}$ e-scooters. Similarly, if $D_i < \Theta^{-}_{v,z}$, the vehicle is only allowed to drop-off D_i e-scooters. As such, by defining $\mathcal{E}_z$ to be the set of ordered directed arcs in zone z resulting from the local routing, a complete feasible solution can be generated by applying Algorithm 1 to obtain the feasible TB. Then, the feasible TC can be computed with the set $\mathcal{E}_z$ and the original variables of

Algorithm 1 Feasible routing and charging.

Initiate variable: $I_{v,i,b} \equiv$ type b inventory level of vehicle v after visiting node i
Initiate variable: TB
for $v \in \mathcal{V}$ **do** $I_{v,0,B} = q'_{v,0,B}$ (initial inventory from hybrid solution)
for $v \in \mathcal{V}$ **do**
  for $z \in \mathcal{Z}$ **do**
    for $e \in \mathcal{E}_z$ **do**
      charge inventory through $e = (i, j)$ with charging function f
      if e-scooters need to be dropped-off at j and $I_{v,j,B} > 0$ **then**
        $d = \arg\min\{I_{v,j,B}, \Theta^{-}_{v,z}, D_j\}$
        update live inventory,$I_{v,j,B} = I_{v,j,B} - d$
        update total benefit, $TB = TB + c_{\text{drop}} \cdot d$
      for $b \in \mathcal{B}$ **do**
        if $\sum_b I_{v,i,b} < Q$ and type b e-scooters need to be picked up at j **then**
          $p = \arg\min\{Q - I_{v,j,b}, \Theta^{+}_{v,z,b}, P_{i,b}\}$
          update live inventory, $I_{v,j,b} = I_{v,j,b} + p$
          update total benefit, $TB = TB + c_{\text{pick},b} \cdot p$

the hybrid model with Eq. (30).

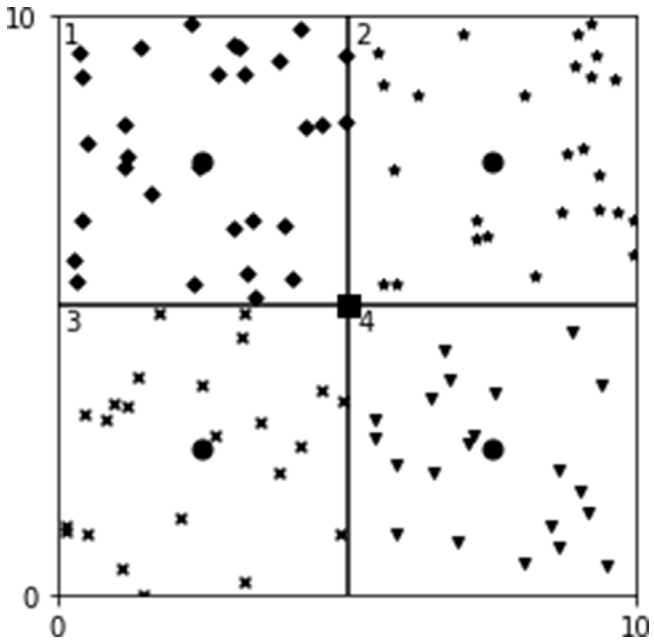

Fig. 5. Example network with 4 zones and 105 nodes where the center square represents the depot and the circles represent waiting locations..

Table 1
Distribution of the number of pickups and drop-offs per zone.

Zone	Drop-off distribution	SoC (%)	Pickup distribution
1	$N(4, 0.5)$	20	$N(1, 0.5)$
		40	$N(2, 0.5)$
		60	$N(1, 0.5)$
2	$N(5, 0.5)$	20	$N(0, 0.5)$
		40	$N(1, 0.5)$
		60	$N(1, 0.5)$
3	$N(2, 0.5)$	40	$N(1, 0.5)$
		60	$N(3, 0.5)$
		80	$N(1, 0.5)$
4	$N(2, 0.5)$	20	$N(0, 0.5)$
		40	$N(1, 0.5)$
		60	$N(1, 0.5)$

4. Numerical tests

The performance of the hybrid model (including the feasible solutions) is tested with hypothetical networks and then compared with the discrete model. Then, the model is applied to the Washington, DC transportation network to show the performance of the model in a real-world instance. All the test cases are run on a computer with 3.40 GHz CPU and 8 GB RAM. The MIP formulations are solved with the CPLEX solver with Python access (called DocPlex). The computation time limit is set to be 1.5 h when $|\mathcal{N}| < 80$, or 3 h otherwise.

4.1. Hybrid vs. discrete

We test the performance of the hybrid model and compare it with that of the discrete one using the same hypothetical networks with similar pickup and drop-off demand. Fig. 5 shows a 10-mile by 10-mile square region which is divided into four contiguous 5-mile by 5-mile square zones. A vehicle starts and ends its tour at the depot located at (5,5) (the black square in Fig. 5), and it is allowed to park at the center of each zone (the black circles in Fig. 5) to enable a longer charging for on-board e-scooters. The coordinates of all the other nodes are generated according to a uniform distribution, and the pickup and drop-off demand at each node is randomly generated according to normal distributions of each zone $N(\bar{D}_z, \sigma_{D_z})$ and $N(\bar{P}_{z,b}, \sigma_{P_{zb}})$, respectively. More details of the demand distributions in each zone are shown in Table 1. The pickup and drop-off demand for all nodes is normalized in each realization to make the total pickup demand equal to the drop-off demand in the entire region (i.e., $\sum_{i\in\mathcal{N}} D_i = \sum_{i\in\mathcal{N}} \sum_{b\in\mathcal{B}} P_{i,b}$).

We also assume that only the e-scooters with SoC> 95% are allowed to be dropped off. For the discrete model, we let $B = 20,\ 50$, and 100, while the last battery level always represents the highest 5% increment; as such, each of the remaining battery levels represents an increment of 5%, $\frac{95}{49}$%, and $\frac{95}{99}$%, respectively.

For the hybrid model, we assume $B = 100$, i.e., each battery level less than 95 represents a $\frac{95}{99}$% increment and the last level represents a 5% increment. We consider two charging functions which, for convenience, are labeled as "slow" and "fast" functions. The "slow" function allows the e-scooters to charge at 1%/min up to an SoC of 80% and then at 0.5%/min afterwards; and the "fast" function doubles both rates but has the same 80% threshold.[6]

The parameters associated with rebalancing vehicles are set as follows: the speed of vehicles $s = 30$ mph, the tour time limit $T = 360$ min, the capacity of vehicles $Q = 25$ e-scooters, the time penalty for stopping at one node $\tau = 1$ min, the lengths of waiting duration allowed at waiting locations $\mathcal{L}_z = \{0, 5, 10, 20, 30, 45, 60\}$ minutes, $\forall z \in \mathcal{Z}$, the fixed cost for deploying a vehicle $c_{\text{veh}} = \$100$/deployment, the travel cost $c_{\text{dist}} = 1$ \$/mile, the unit cost of having nonempty on-board inventory at the beginning of the tour $c_{\text{extra}} = 1$ \$/e-scooter, the revenue for dropping off an e-scooter $c_{\text{drop}} = 10$ \$/e-scooter, and the benefit for picking up a type b e-scooter is $c_{\text{pick},b} = 4, 3, 2, 1$ \$/e-scooter for e-scooters with SoC = 20%, 40%, 60%, and 80%, respectively.[7] All cases are solved when only one rebalancing vehicle is available, so as to better compare solution quality and computation efficiency across all scenarios.

We selected six test network sizes with $|\mathcal{N} \cup O \cup S| \in \{15, 30, 55, 80, 105, 115\}$. For each network size, three instances are randomly generated and solved for a total of 18 cases by applying both the hybrid and discrete models. The average results across three instances for each network size are presented in Table 2 for the hybrid model, and Table 3 for the discrete model, which include the average objective values, the average vehicle distance traveled, the average proportion of fulfilled demand, the average CPU time and the MIP gap for the discrete model. The "Heuristic 1" and "Heuristic 2" columns report the results from the two heuristic methods described in Section 3.2.3, while the "Estimate" column only reports the approximated CA estimate produced by the hybrid model alone. Moreover, for the distance traveled, only the CA estimate and "Heuristics 1&2" are reported because the same routing decisions are used in the CA heuristic 1 and heuristic 2 solutions.

The results in Tables 2 and 3 clearly show the superior performance of the hybrid model over the discrete MIP approach in terms of solution quality and computation time, especially when the number of nodes is larger than 55. For the largest instance, the hybrid model is able to produce reasonable solutions in about 5% of the computation time, as compared to the discrete counterpart (for $B = 20$), while still producing higher objective values for both the fast and slow charging functions. For the larger cases (e.g., those with $B = 50$ and $B = 100$), the MIP solver could not find even a feasible solution within the time limit of 3 h.

Fig. 6 plots the average objective function values for different test instances. Only the results with $B = 20$ is plotted to portray the trend of discrete solutions; however Table 3 shows that for cases with 55 and 80 nodes, the discrete model can produce slightly higher objective values when the number of battery levels is 50 and 100. Fig. 6 shows that, for both charging rate functions, the hybrid model yields strictly better solutions when the number of nodes is greater than 55. Such results is expected, as the CA method builds upon asymptotic results for large networks. Moreover, we also observe that the hybrid model can produce comparable solutions to the discrete model even for a small number of nodes. Fig. 6 also shows that the CA estimat is affected by both the number of nodes and the charging rate. For both slow and fast charging functions tested, the gaps between the CA estimation and the CA heuristic solutions grow slowly as the number of nodes increases. Furthermore, Fig. 6b shows that for a faster charging rate, the CA estimation can better approximate the CA heuristic 1 solution (with an average relative error of 1.9%) than when the charging rate is slow (with an average relative error of 6.6%). For the slow charging function, the gaps between the CA estimate and the CA heuristics 1 & 2 solutions get wider as the number of nodes increases. This phenomenon may be due to the conservative charging performed by the transition function f. For every arc traversed by the vehicle, there is a fraction of the charging time which is lost because the function f does not account for partial charging between two battery levels b and $b+1$ (e.g., see Fig. 1). The transition function f accumulates this small error for every node and for every battery level $b < B$ until the e-scooters transition to type B e-scooters. Once e-scooters transition into type B e-scooters, no error is accumulated because no further transitions are performed. Hence, the more nodes a vehicle must visit in the local route and the slower the charging rate, the larger the charging error. This may explain why both a slower charging rate and higher number of nodes in each zone are associated with a larger error between the estimate and either heuristic solution. The heuristic 2 solution is shown to always produce a lower value as compared to the CA heuristic 1 solution. This sacrifice of optimality comes with benefits regarding the computation time since the longest it took to produce a solution was 570 s (i.e., with 115 nodes), while it took over 1 h to produce the solution with CA heuristic 1.

[6] Our choice of charging rate is somewhat arbitrary. Yet, companies such as StoreDot and GBatteries are starting to develop ultra-fast charging technologies specifically for electric vehicles which can charge e-scooters between 5 to 10 min (StoreDot, 2020; GBatteries, 2020). We suspect that onboard charging capabilities of similar efficiency would be available in the near future.

[7] The value of parameter c_{veh} includes driver's wage for $T = 6$ h of operation per day, at \$14/h, plus the prorated daily cost of about \$16 for depot/equipment maintenance and operations; the latter is estimated based on an annual cost of about \$6000 for a charging station (Smith and Castellano, 2015). The value of c_{dist} is prorated from a total life cycle cost of \$80,000 for a light commercial electric vehicle that runs 80,000 miles in 8 years, based on information in Lebeau et al. (2019). The values of other parameters such as c_{extra} and $c_{\text{pick},b}$ are based on our best guesses due to lack of real-world data; however, the validity of our models does not depend on their specific values.

Table 2
Average results of the hybrid model from numerical experiments varying the charging rate and number of nodes.

Charging function	Number of nodes	Objective			Distance traveled (mi)		Fulfilled demand (%)			CPU time (s)		
		Estimate	Heuristic 1	Heuristic 2	Estimate	Heuristics 1&2	Estimate	Heuristic 1	Heuristic 2	Estimate	Heuristic 1	Heuristic 2
slow	15	145.4	159.0	134.7	55.3	44.4	99.5	100	93.0	64	101	64
	30	554.4	549.2	463.7	68.6	71.7	93.0	92.3	83.3	39	131	51
	55	940.9	931.5	777.1	84.9	88.6	71.3	70.7	62.0	377	597	381
	80	1162.9	1120.3	871.2	97.6	106.3	59.0	55.7	47.0	435	825	507
	105	1476.0	1281.7	948.6	108.2	115.5	55.0	48.0	39.3	100	981	221
	115	1427.3	1294.5	1079.6	112.3	120.3	49.3	45.0	39.3	352	3800	500
fast	15	145.7	149.7	120.2	55.3	49.7	100	100	89.7	8	45	8
	30	585.9	577.8	475.4	68.6	70.9	97.0	96.3	83.7	13	105	22
	55	1137.1	1115.6	979.8	89.9	87.2	83.3	82.3	75.0	45	264	47
	80	1579.8	1637.7	1298.5	97.6	102.1	75.3	76.7	64.0	14	404	223
	105	2023.2	2021.2	1660.5	108.2	113.1	71.3	70.3	59.7	117	997	143
	115	2203.6	2249.2	1784.9	112.3	120.3	70.1	70.7	58.3	251	3699	570

Table 3
Average results of the discrete model from numerical experiments with varying charging rate, number of battery levels and number of nodes.

Charging function	Number of nodes	Objective			Distance traveled (mi)			Fulfilled demand (%)			CPU time (s)			Gap		
		Number of Battery Levels														
		20	50	100	20	50	100	20	50	100	20	50	100	20	50	100
slow	15	156.4	156.0	151.9	43.2	43.9	45.8	100.0	100.0	100.0	817	746	1493	0.72	0.73	0.75
	30	576.5	577.4	561.2	83.9	90.2	99.3	99.0	99.3	99.0	4490	1293	973	0.26	0.26	0.30
	55	765.6	927.7	1029.4	96.5	132.7	141.3	63.0	75.7	84.0	5993	9488	10,228	0.94	0.60	0.44
	80	733.3	807.7	–	104.4	114.7	–	40.0	43.7	–	8100	10,154	–	2.07	1.81	–
	105	501.7	423.4	–	106.5	92.8	–	21.3	20.0	–	10,740	10,800	–	9.16	6.10	–
	115	614.9	–	–	135.2	–	–	25.0	–	–	10,490	–	–	4.42	–	–
fast	15	156.6	158.8	153.9	44.7	42.7	45.0	100.0	100.0	100.0	400	474	1325	0.72	0.70	0.73
	30	596.3	600.2	598.1	73.4	68.6	71.4	99.3	99.3	99.5	1330	1777	1401	0.22	0.21	0.22
	55	1237.3	1266.6	1221.2	138.0	139.2	120.8	96.7	97.7	92.0	6995	7115	10,567	0.20	0.17	0.22
	80	1257.7	1508.6	–	113.1	132.6	–	63.7	74.7	–	6594	10,428	–	0.84	0.50	–
	105	1178.3	–	–	126.8	–	–	45.5	–	–	10,153	–	–	1.64	–	–
	115	718.4	–	–	90.6	–	–	27.0	–	–	10,778	–	–	4.74	–	–

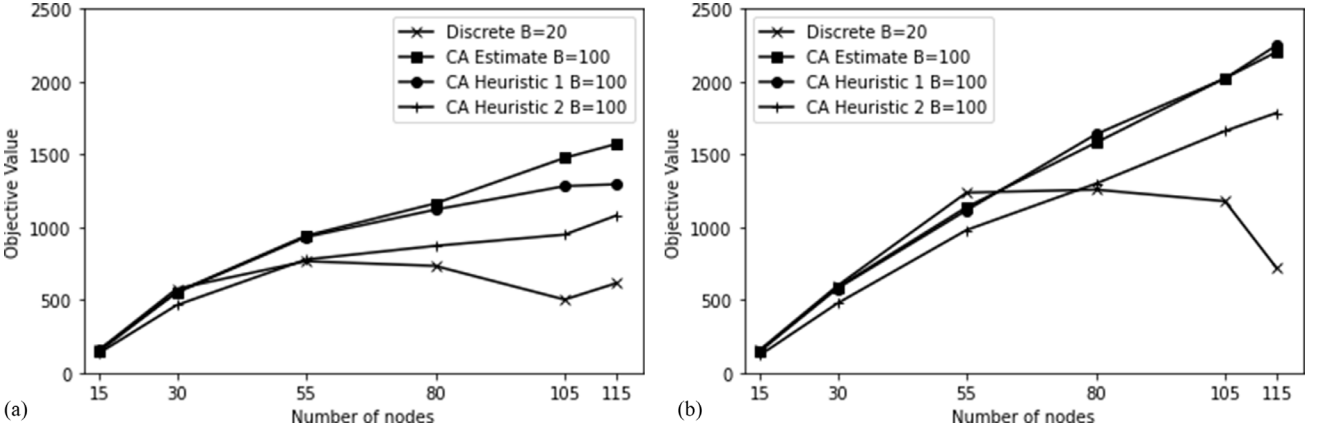

Fig. 6. Algorithm comparison under (a) the "slow" charging rate and (b) the "fast" charging rate ($B = 20$ for the discrete model and $B = 100$ for the hybrid model).

Table 4
Objective value comparison as a function of the number of zones.

Number of zones	Objective			CPU time (s)		
	CA Estimate	CA Heuristic 1	CA Heuristic 2	CA Estimate	CA Heuristic 1	CA Heuristic 2
4	3961.4	3798.5	3191.2	1	1838	447
5	4147.6	3852.8	3433.3	3	5537	361
6	4163.1	3897.1	3478.9	18	14,864	561
7	4083.6	3818.2	3333.6	126	18,381	741
8	4043.87	3946.8	3306.3	164	20,003	519

Regarding the distance traveled, the hybrid model tends to produce a similar or lower distances when the number of nodes is 30 or greater. The are some scattered exceptions when the number of nodes is greater than 80, but for those cases Fig. 6 shows that the objective value of the discrete model is significantly lower as compared to both the CA heuristics.

4.2. Zone partitioning

In order to test the influence of zone partition on solution quality and computation time, the 200-node network presented in Fig. 5 was solved by further partitioning the original 4 zones, incrementally, into 8. Each partition is done by applying the k-means clustering algorithm from the scikit-learn package with Python (Pedregosa et al., 2011). The 5-zone case is produced by splitting zone 1 into two equal zones; the 6-zone case is produced by further splitting zone 2 into two; and so on. Furthermore, To make the results comparable, no waiting was allowed at the zone centroids, otherwise the vehicles would have had an extra centroid to wait, and the objective value would easily increase with the addition of zones.

Table 4 shows the objective values for the CA estimate, the CA heuristic 1 solution, and the CA heuristic 2 solution. It is shown that the CA estimate increases by at most 5%, the CA heuristic 1 solution by 4%, and the CA heuristic 2 solution by 9%, as compared to the corresponding solutions with 4 zones. Even when waiting is not allowed at centroids, the solution quality is always improved (as compared to 4 zones), because extra flexibility in vehicle routing always results on improvement in the objective value. However, this improvement in objective value comes at a cost in solution time, as the CPU time required to generate the heuristic 1 solution significantly increases with the number zones. In contrast, for the CA heuristic 2 solution, the CPU time increase is moderate (within 300 s).

4.3. Case study: Washington, DC

In this section, we implement the hybrid model for a real-world e-scooter system in Washington, DC, which involves a significantly greater number of nodes. The municipal is divided into 392 traffic analysis zones (TAZ) and 8 historical wards with definite boundaries, as shown in Fig. 7. For simplicity, the centroid of each TAZ is treated as a discrete demand node while each of the 8 wards is considered as one of zones in the proposed hybrid model. As such, there are 30, 83, 49, 71, 45, 52, 71, and 39 nodes in zones 1 through 8, respectively. A depot is assumed to be located outside of the city limits in the Northeast area and is illustrated as a square in Fig. 7. McKenzie (2019) made a spatiotemporal analysis of the demand pattern of e-scooters by analyzing data from the company Lime, and showed that most demand originates from zones 1, 2, and 6, while the rest of the zones have relatively lower trip density. Following this pattern of trips, two scenarios are evaluated: (i) the pickup and drop-off demands in each zone are more or less balanced, and (ii) zones 1, 2, and 6 (i.e., downtown area) have the majority of the pick-up demand, while the surrounding zones 3, 4, 5, 7, and 8 have predominately the drop-off demand. Due to the large problem size, only CA heuristic 2 is applied, and the computation time limit is set to be 3600 sec.

We again use $B = 100$ battery levels and the pickup and drop-off demands for each node are generated with the same procedure as in the previous section. As such, the distributions in Table 5 are used for the two scenarios. It is assumed that e-scooters have, at most, a SoC of 60%. In both scenarios, the randomly generated demand data are normalized to fit a total fleet size of 750 e-scooters (which resembles the real-world fleet size data posted on the Washington DC government website District Department of Transportation, 2020), and the total amounts of expected pickup and drop-off demands in the DC area are the same. The model is solved for three different vehicle capacities $Q \in \{20, 30, 40\}$, for initial charging rates 1%/min, 2%/min, and 3%/min for SoC less than 80% (and half the rate for SoC exceeding 80%), and for 3 different SoC ranges for the "full" battery level $b = B$, 10%, 5%, and 1% (i.e., e-scooters with SoC greater than 90%, 95%, and 99% can be dropped off, respectively). The other parameters are set as follows: $T = 600$ min, $\tau = 3$ min, $s = 30$ mph, $c_{\text{pick},b} = \$3$/e-scooter for e-scooters with SoC$\leq$ 20%, or $c_{\text{pick},b} = \$2$/e-scooter for e-scooters with 20% <SoC$\leq$ 40%, or $c_{\text{pick},b} = \$1$/e-scooter for e-scooters with 40% <SoC$\leq$ 60%, and $c_{\text{drop}} = \$15$/e-scooter.[8] All cases are solved while enforcing usage of exactly three rebalancing vehicles, so as to better compare the impacts of other parameters.

The results of scenario 1, as presented in Table 6, confirm our expectation that the charging rate has a strong but diminishing marginal influence on the amount of fulfilled demand. All cases solved with a charging rate of 2%/min have, on

[8] Some of the parameter values are slightly different from those in Section 4.1, so as to test variability of model inputs.

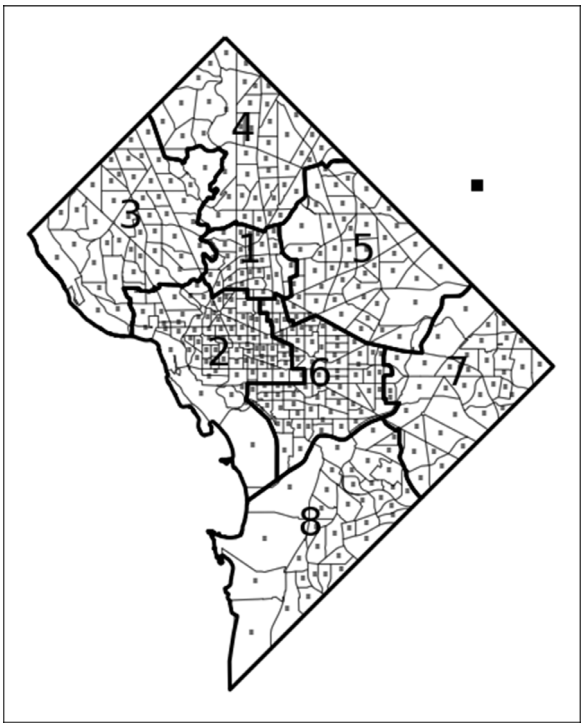

Fig. 7. Washington DC map with the TAZ centroids as nodes.

Table 5
Distribution of the number of pickups and drop-offs per zone in the Washington, DC case study.

Zone	Drop-off distribution		SoC (%)	Pickup distribution	
	Scenario 1	Scenario 2		Scenario 1	Scenario 2
1	$N(3, 0.4)$	$N(0, 0.4)$	20	$N(1, 0.5)$	$N(1, 0.5)$
			40	$N(2, 0.5)$	$N(2, 0.5)$
2	$N(3, 0.4)$	$N(0, 0.4)$	20	$N(2, 0.5)$	$N(2, 0.5)$
			40	$N(1, 0.5)$	$N(1, 0.5)$
3	$N(1, 0.4)$	$N(1, 0.4)$	40	$N(1, 0.5)$	$N(0, 0.5)$
			60	$N(0, 0.5)$	$N(0, 0.5)$
4	$N(1, 0.4)$	$N(1, 0.4)$	20	$N(0, 0.5)$	$N(0, 0.5)$
			40	$N(1, 0.5)$	$N(0, 0.5)$
5	$N(2, 0.4)$	$N(2, 0.4)$	20	$N(1, 0.5)$	$N(0, 0.5)$
			40	$N(1, 0.5)$	$N(0, 0.5)$
6	$N(2.5, 0.4)$	$N(2.5, 0.4)$	20	$N(1, 0.5)$	$N(1, 0.5)$
			40	$N(1, 0.5)$	$N(1, 0.5)$
7	$N(1, 0.4)$	$N(1, 0.4)$	20	$N(0.5, 0.5)$	$N(0, 0.5)$
			40	$N(1, 0.5)$	$N(0, 0.5)$
8	$N(1, 0.4)$	$N(1, 0.4)$	20	$N(0.5, 0.5)$	$N(0, 0.5)$
			60	$N(1, 0.5)$	$N(0, 0.5)$

average, a 23.9% increase in fulfilled demand as compared to the cases solved with a rate of 1%/min. On the other hand, the cases solved with a charging rate of 3%/min have, on average, only an additional 6.9% improvement over the cases solved with a rate of 2%/min. The carrying capacity of the vehicles also seems to have a great influence, especially when the charging rates are low (i.e., probably because the e-scooters have to stay in the vehicles longer to be charged). For the charging rate of 1%/min, increasing the capacity of the vehicles from 20 to 30 and 30 to 40, on average, increases the fulfilled demand by 12.5% and 9.9%, respectively. For higher charging rates, increasing the capacity from 20 to 30 and 30 to 40 only improves the demand by 5.9% and 2.9%, respectively. In contrast, the SoC range of the "full" battery level $b = B$ has the least influence. The fulfilled demand increases by only an average of 2.5% when the range is increased from 1% to 5%, and another 3.2% when it is increased from 5% to 10%.

Table 7 shows that the capacity of vehicles and the charging rate remain as the two most influential parameters in scenario 2. However, it should be noted that, unlike scenario 1, the marginal benefit for employing a larger size vehicle

Table 6
Results from scenario 1 of the DC case study.

Charging rate (%/min)	Range for $b = B$ (%)	Capacity	Objective		Fulfilled demand	CPU Time
			CA Estimate	CA Heuristic 2	CA Heuristic 2	CA Heuristic 2
1	1	20	5050.0	4271.0	38.4	2270
		30	6783.6	5550.2	47.3	2024
		40	8860.0	7412.1	61.3	2167
	5	20	5894.0	4828.3	42.5	2314
		30	7844.0	6340.3	53.3	2294
		40	9325.8	7808.6	64.8	2274
	10	20	6198.2	5506.3	47.0	2157
		30	8901.5	7829.2	65.0	2263
		40	9847.8	8402.7	69.3	2151
2	1	20	9077.7	8227.6	67.7	2289
		30	11037.9	9531.2	77.8	2228
		40	11490.3	10127.6	83.0	2286
	5	20	9840.5	8715.0	70.9	2290
		30	11255.6	9935.7	80.6	2344
		40	11498.3	10083.7	82.0	2288
	10	20	10349.3	9274.7	75.3	1971
		30	11625.0	10159.2	82.9	2325
		40	11710.9	10325.7	84.2	2264
3	1	20	11181.2	10027.1	81.5	2277
		30	11551.9	10312.9	84.1	2095
		40	11912.8	10701.0	87.9	2233
	5	20	11518.3	10238.3	83.3	2028
		30	11734.4	10453.1	85.3	2036
		40	12066.5	10783.6	88.5	2025
	10	20	11455.1	10114.0	82.2	2188
		30	11956.8	10511.1	85.8	2234
		40	12132.2	10785.2	88.5	2322

Table 7
Results from scenario 2 of the DC case study.

Charging rate (%/min)	Range for $b = B$ (%)	Capacity	Objective		Fulfilled demand	CPU Time
			CA Estimate	CA Heuristic 2	CA Heuristic 2	CA Heuristic 2
1	1	20	4668.9	3636.4	32.3	2882
		30	6086.1	4539.1	39.3	2760
		40	6977.8	5844.7	49.6	3078
	5	20	4944.0	3838.9	34.0	2980
		30	6229.8	4787.9	41.0	2922
		40	6592.4	4906.9	42.9	2756
	10	20	5405.0	4258.4	37.4	2742
		30	6790.1	5364.5	45.6	3000
		40	7518.7	6079.5	51.0	2957
2	1	20	6399.9	5280.6	44.8	1990
		30	7280.5	5623.8	47.8	2168
		40	8110.7	6514.2	55.0	2295
	5	20	6862.7	5927.6	50.0	1804
		30	7849.3	6620.3	55.6	2030
		40	8470.8	7502.0	63.1	2050
	10	20	6953.3	6023.1	50.7	1903
		30	7897.5	6608.2	55.5	2072
		40	8517.5	7399.7	62.2	2011
3	1	20	7201.6	6240.2	52.6	2984
		30	7761.5	6567.8	55.4	2507
		40	8480.8	7415.1	62.5	2667
	5	20	6759.8	5692.0	48.0	2815
		30	7918.8	6847.4	57.7	3011
		40	8480.8	7362.4	62.0	2068
	10	20	7211.8	6015.6	50.7	2789
		30	8046.7	6711.7	56.5	2998
		40	8599.4	7355.4	62.0	2910

tends to increase when the charging rate is high. For the charging rate of 1%/min, the marginal improvement for increasing the capacity from 20 to 30 and 30 to 40 are 7.4% and 5.9%, respectively, while for higher charging rates, increasing the capacity of vehicles from 20 to 30 and 30 to 40 have a marginal improvement of 5.3% and 6.4%, respectively. The reasons behind this might be that, if the pickup and drop-off demands are unevenly distributed across zones as in scenario 2, the vehicle capacity may become a extremely restrictive factor for line-haul shipments when the charging rates are high, such that increasing its magnitude may result in greater improvements. Therefore, agencies should be encouraged to use large vehicles if they can, as long as the marginal benefit exceeds the cost difference, especially for the cases that are similar to those in scenario 2. In addition, it is also interesting to observe from the table that the agencies should charge the e-scooters to 100% SoC whenever possible. This is probably because charging an extra 5% (i.e., either from a SoC of 90% to 95% or 95% to 100%) only takes the trucks a short time (between 3.33 and 10 min, depending on the charging rate). This time can easily be absorbed into the tours either through the line-haul trips or extra waiting at depots.

Finally, we can observe that, under the same total amount of expected demand and the same zone configuration, there is a significant difference of 25.4% between the highest proportions of fulfilled demand in scenarios 1 and 2. This indicates that the pickup and drop-off demand distributions across zones can greatly influence the performance of the rebalancing and charging operations. In scenario 2, the majority of the pickup demand is concentrated in the downtown zones 1, 2, and 6, which means that the vehicles entering those zones are in charge of fulfilling most of the drop-off demand in the surrounding zones. This turns to be very limiting as the pickup demand within each of these three downtown zones easily surpasses the capacity of vehicles, even when the capacity is set to 40 – the trucks would have to make many interzonal trips to complete pickup and drop-off services. One possible way of enhancing the performance of the rebalancing and charging operations in scenario 2 is to increase the number of zones (e.g., by splitting a large zone into multiple smaller zones), such that the network (with our operational setting) can have a greater number of idling locations. In this way, the vehicle capacity becomes a less restrictive factor when serving high demand zones. However, in practice, the choices of these settings (e.g., zone partition) must be made on a case-by-case basis according to the demand distributions as well as considerations over computational efficiency vs. solution quality.

5. Conclusion

E-scooter sharing systems come with its unique logistical challenges as compared to the widely studied bike rebalancing problem. This is due to the extra dimension of complexity added by e-scooter charging. This paper presents ES-RCP with on-board charging decisions, and develops a mixed integer programming formulation. The SoC of e-scooters is discretized into a finite number of battery levels. Battery at each SoC level is treated as a separate commodity, and the various types of batteries are linked through a transition function (which depends on the charging capabilities of rebalancing vehicles). The mixed integer programming formulation is extremely difficult to solve. Then, a discrete-continuous hybrid model is introduced by decomposing the routing plan of vehicles into local tours and line-haul trips in order to decrease the size of the problem and handle large scale instances. Two heuristics methods are proposed in order to generate feasible solutions. CA heuristic 1 generally produces higher quality solutions but it requires a significantly longer computation time, while CA heuristic 2 can produce reasonable solutions in a very short time. Numerical experiments demonstrated that these heuristic methods (especially heuristic 2) with hybrid CA modeling approach produce better solutions for large networks very fast (e.g., in under 6% of the time it takes to solve the discrete model directly). On the other hand, experiments also show that the CA estimate closely approximates the feasible solution from heuristic 1. Moreover, the charging function is shown to affect the quality of the hybrid model estimation as compared to the feasible solutions. In the hypothetical networks, a faster charging rate produce a better estimation while a slow one leads to a significantly greater difference between the CA estimation and the feasible solutions from both heuristic methods. To demonstrate the capabilities of the hybrid model in the real world, the regional system in Washington, DC is used as a case study under two demand scenarios. For scenario 1 in which the pickup and drop-off demands are similar in each zone, the charging rate has the most influence on the fulfilled demand. In scenario 2, in which the pickup demand is concentrated on the downtown area, the vehicle capacity, along with the charging rate are both found to be influential parameters.

Future research can be conducted in several directions. The size of the e-scooters allow for rebalancing vehicles to carry a great number of e-scooters, so in practice, the restrictive factor in the rebalancing operations may not be the capacity of the vehicles. Instead, it is more likely to be the charging capabilities of the vehicle (e.g., the battery size as well as the maximum number of e-scooters that can be charged simultaneously). The battery could be a significant factor on the service and may limit the size and the number of zones a vehicle can serve. This is natural extension of this paper and will be left for future work. The model can also be extended to exploit the dock-less property of e-scooter service so that pickups and drop-offs can occur anywhere in a zone. Additionally, this work assumes overnight operations and does not consider the dynamic case in which e-scooter user trips and traffic conditions can affect the operator's decisions. Therefore, another extension of this work is to consider the dynamic rebalancing operations during the day. Finally, it would be interesting to explore other application contexts of this model; e.g., the routing of line-haul trucks in truck-drone deliveries, where a group of drones must be sufficiently charged on board of the truck before they can be deployed for last-mile deliveries.

Declaration of Competing Interest

The authors declare that there is no conflict of interest.

CRediT authorship contribution statement

Jesus Osorio: Conceptualization, Methodology, Validation, Software, Data curation, Writing - original draft. **Chao Lei:** Conceptualization, Methodology, Validation, Writing - original draft. **Yanfeng Ouyang:** Conceptualization, Methodology, Validation, Supervision, Funding acquisition, Writing - review & editing.

Acknowledgments

The helpful comments from the editors and three anonymous reviewers are gratefully acknowledged. This research was supported in part by the U.S. National Science Foundation via Grant CMMI-1662825. The second author was a postdoctoral research associate at Illinois while the majority of this research was conducted. His efforts after joining Shanghai Maritime University were partially supported by the National Natural Science Foundation of China via Grant no. 72001136.

Appendix A. Notation

The following is a list of all mathematical notation utilized throughout the paper.

Parameters

$\mathcal{A}$	set of arcs
$\mathcal{B}$	set of battery levels
$\mathcal{C}_{b,i,j,l}$	set of battery levels which transition up to b after traversing arc (i, j) and waiting l units of time
$\mathcal{C}'_{z,b}$	set of battery levels which transition up to b after local tour in zone z
$\mathcal{E}_z$	set of ordered arcs resulting from the local routing in zone z
$\mathcal{L}_i$	set of waiting times allowed at node i
$\mathcal{M}$	subset of nodes where vehicles are allowed to wait
$\mathcal{N}$	set of demand nodes
$\mathcal{V}$	set of vehicles
$\mathcal{Z}$	set of zones
a_z	area size of zone z [mile^2]
c_{drop}	benefit of dropping off a type B e-scooter [$/drop-off]
$c_{\text{pick},b}$	benefit of picking up a type b e-scooter [$/type b pickup]
c_{veh}	fixed cost of deploying a vehicle [$/vehicle deployment]
c_{dist}	cost per unit of distance [$/mile]
c_{extra}	penalty per e-scooter for having non-zero inventory in the beginning of the tour [$/e-scooter]
D_i	drop-off demand at node i
$\tilde{D}_z$	average drop-off demand per node in zone z [e-scooters/node]
d_{ij}	travel distance from node i to node j [mile]
B	highest battery level representing sufficiently charged e-scooters ready for drop-off
f	transition function for e-scooter battery levels
k	dimensionless constant
M	large number
O	depot where vehicles start their tours
$P_{i,b}$	number of type b e-scooters available for pickup at node i
$\tilde{P}_{z,b}$	average pickup demand of type b e-scooters per node in zone z [e-scooters/node]
Q	load capacity of vehicles
T	time limit of vehicle tours [min]
r_b	time during the local tour in which type b e-scooters become type B [min]
S	depot where vehicles end their tours
s	speed of vehicles [mph]
t_{ij}	travel time from node i to node j [min]
TB	total benefit of rebalancing operations [$/day]
TC	total cost of rebalancing operations [$/day]
Δ_z	node density of zone z
Γ_{ij}	charging duration from node i to node j [min]
$\lambda_{z,b,b'}$	proportion of type b e-scooters picked up in zone z which become type b' at the end of the tour
Π_z	local tour time estimate in zone z [min]

τ pickup/drop-off duration [min]

Variables

$q_{v,i,b}$ number of type b e-scooters on board when vehicle v arrives at node (zone) i
$q'_{v,z,b}$ number of type b e-scooter on board after vehicle v serves zone z
$u_{v,i}$ arrival time of vehicle v at node (zone) i [min]
$x_{v,i,j,l}$ binary variable which equals 1 if vehicle v travels from node (zone) i to node (zone) j and waits l units of time
$\theta^{+}_{v,i,b}$ type b e-scooters picked up by vehicle v at node i
$\theta^{-}_{v,i}$ type B e-scooters dropped of by vehicle v at node i
$\Theta^{+}_{v,z,b}$ average number of type b e-scooters picked up per node in zone z by vehicle v
$\Theta^{-}_{v,z}$ average number of type B e-scooters dropped off per node in zone z by vehicle v

References

Ait-Ouahmed, A., Josselin, D., Zhou, F., 2018. Relocation optimization of electric cars in one-way car-sharing systems: modeling, exact solving and heuristics algorithms. Int. J. Geograph. Inf. Sci. 32 (2), 367–398. doi:10.1080/13658816.2017.1372762.

Alvarez-Valdes, R., Belenguer, J.M., Benavent, E., Bermudez, J.D., Muñoz, F., Vercher, E., Verdejo, F., 2016. Optimizing the level of service quality of a bike-sharing system. Omega 62, 163–175. doi:10.1016/j.omega.2015.09.007.

Ansari, S., Başdere, M., Li, X., Ouyang, Y., Smilowitz, K., 2018. Advancements in continuous approximation models for logistics and transportation systems: 1996–2016. Transp. Res. Part B 107, 229–252. doi:10.1016/j.trb.2017.09.019.

Barabonkov, D., D'Alonzo, S., Pierre, J., Kondor, D., Zhang, X., Tien, M. A., 2020. Simulating and Evaluating Rebalancing Strategies for Dockless Bike-Sharing Systems. arXiv:2004.11565[physics]

Beardwood, J., Halton, J.H., Hammersley, J.M., 1959. The shortest path through many points. Math. Proc. Cambridge Philos. Soc. 55 (4), 299–327. doi:10.1017/S0305004100034095.

Brandstätter, G., Gambella, C., Leitner, M., Malaguti, E., Masini, F., Puchinger, J., Ruthmair, M., Vigo, D., 2016. Overview of Optimization problems in electric car-sharing system design and management. In: Dawid, H., Doerner, K.F., Feichtinger, G., Kort, P.M., Seidl, A. (Eds.), Dynamic Perspectives on Managerial Decision Making, Vol. 22. Springer International Publishing, Cham, pp. 441–471. doi:10.1007/978-3-319-39120-5_24.

Brinkmann, J., Ulmer, M.W., Mattfeld, D.C., 2015. Short-term strategies for stochastic inventory routing in bike sharing systems. Transp. Res. Procedia 10, 364–373. doi:10.1016/j.trpro.2015.09.086.

Bruglieri, M., Colorni, A., Luè, A., 2014. The vehicle relocation problem for the one-way electric vehicle sharing: an application to the milan case. Procedia - Soc. Behav. Sci. 111, 18–27. doi:10.1016/j.sbspro.2014.01.034.

Buchmann, I., 2020. Fast and Ultra-fast Chargers - Battery University. https://batteryuniversity.com/learn/article/ultra_fast_chargers.

Caggiani, L., Camporeale, R., Ottomanelli, M., 2017. A dynamic clustering method for relocation process in free-floating vehicle sharing systems. Transp. Res. Procedia 27, 278–285. doi:10.1016/j.trpro.2017.12.146.

Caggiani, L., Camporeale, R., Ottomanelli, M., Szeto, W.Y., 2018. A modeling framework for the dynamic management of free-floating bike-sharing systems. Transp. Res. Part C 87, 159–182. doi:10.1016/j.trc.2018.01.001.

Caggiani, L., Ottomanelli, M., 2012. A modular soft computing based method for vehicles repositioning in bike-sharing systems. Procedia - Soc. Behav. Sci. 54, 675–684. doi:10.1016/j.sbspro.2012.09.785.

Chemla, D., Meunier, F., Wolfler Calvo, R., 2013. Bike sharing systems: solving the static rebalancing problem. Discrete Optim. 10 (2), 120–146. doi:10.1016/j.disopt.2012.11.005.

Daganzo, C., 2005. Logistics Systems Analysis, fourth ed. Springer, Berlin ; New York.

Daganzo, C., Ouyang, Y., 2019. Public Transportation Systems:Principles of System Design, Operations Planning and Real-Time Control. World Scientific.

Daganzo, C.F., 1984. The distance traveled to visit *N*points with a maximum of *C*stops per vehicle: an analytic model and an application. Transp. Sci. 18 (4), 331–350. doi:10.1287/trsc.18.4.331.

Daganzo, C.F., 1984. The length of tours in zones of different shapes. Transp. Res. Part B 18 (2), 135–145. doi:10.1016/0191-2615(84)90027-4.

Dell'Amico, M., Hadjicostantinou, E., Iori, M., Novellani, S., 2014. The bike sharing rebalancing problem: mathematical formulations and benchmark instances. Omega 45, 7–19. doi:10.1016/j.omega.2013.12.001.

District Department of Transportation, 2020. Dockless vehicle permits in the district. Dockless Vehicle Permits in the District.

Domonoske, C., 2019. Who charges all those electric scooters? Follow a nocturnal 'juicer'. https://www.mprnews.org/story/2019/03/13/npr-who-charges-all-those-electric-scooters-follow-a-nocturnal-juicer.

Elkins, K., 2019. You can make hundreds of dollars a day charging electric Scooters—Here's how. https://www.cnbc.com/2019/05/22/how-to-make-money-charging-electric-scooters.html.

Erdoğan, G., Battarra, M., Wolfler Calvo, R., 2015. An exact algorithm for the static rebalancing problem arising in bicycle sharing systems. Eur. J. Oper. Res. 245 (3), 667–679. doi:10.1016/j.ejor.2015.03.043.

Fan, R.-N., Ma, F.-Q., Li, Q.-L., 2020. Optimization strategies for dockless bike sharing systems via two algorithms of closed queuing networks. Processes 8 (3), 345. doi:10.3390/pr8030345.

Forma, I.A., Raviv, T., Tzur, M., 2015. A 3-step math heuristic for the static repositioning problem in bike-sharing systems. Transp. Res. Part B 71, 230–247. doi:10.1016/j.trb.2014.10.003.

Gambella, C., Malaguti, E., Masini, F., Vigo, D., 2018. Optimizing relocation operations in electric car-sharing. Omega 81, 234–245. doi:10.1016/j.omega.2017.11.007.

GBatteries, 2020. GBatteries - Ultra-fast charging without compromising cycle life. https://www.gbatteries.com/.

Griswold, A., 2019. Shared scooters don't last long. https://qz.com/1561654/how-long-does-a-scooter-last-less-than-a-month-louisville-data-suggests/.

Ha, K., 2019. Bird Charger and Lime Juicer - Side Hustling As An Electric Scooter Charger. https://financialpanther.com/bird-charger/.

Hajibabai, L., Ouyang, Y., 2016. Planning of resource replenishment location for service trucks under network congestion and routing constraints. Transp. Res. Rec. 2567 (1), 10–17. doi:10.3141/2567-02.

Hall, R.W., 1985. Determining vehicle dispatch frequency when shipping frequency differs among suppliers. Transp. Res. Part B 19 (5), 421–431. doi:10.1016/0191-2615(85)90055-4.

Hernández-Pérez, H., Salazar-González, J.-J., 2003. The one-commodity pickup-and-delivery travelling salesman problem. In: Goos, G., Hartmanis, J., van Leeuwen, J., Jünger, M., Reinelt, G., Rinaldi, G. (Eds.), Combinatorial Optimization — Eureka, You Shrink!, 2570. Springer Berlin Heidelberg, Berlin, Heidelberg, pp. 89–104. doi:10.1007/3-540-36478-1_10.

Hernández-Pérez, H., Salazar-González, J.-J., 2014. The multi-commodity pickup-and-delivery traveling salesman problem. Networks 63 (1), 46–59. doi:10.1002/net.21521.

Ho, S.C., Szeto, W., 2014. Solving a static repositioning problem in bike-sharing systems using iterated tabu search. Transp. Res. Part E 69, 180–198. doi:10.1016/j.tre.2014.05.017.

Ho, S.C., Szeto, W., 2017. A hybrid large neighborhood search for the static multi-vehicle bike-repositioning problem. Transp. Res. Part B 95, 340–363. doi:10.1016/j.trb.2016.11.003.

Illgen, S., Höck, M., 2019. Literature review of the vehicle relocation problem in one-way car sharing networks. Transp. Res. Part B 120, 193–204. doi:10.1016/j.trb.2018.12.006.
Kloimüllner, C., Papazek, P., Hu, B., Raidl, G.R., 2014. Balancing bicycle sharing systems: an approach for the dynamic case. In: Blum, C., Ochoa, G. (Eds.), Evolutionary Computation in Combinatorial Optimisation, 8600. Springer Berlin Heidelberg, Berlin, Heidelberg, pp. 73–84. doi:10.1007/978-3-662-44320-0_7.
Labadi, K., Benarbia, T., Barbot, J.-P., Hamaci, S., Omari, A., 2015. Stochastic petri net modeling, simulation and analysis of public bicycle sharing systems. IEEE Trans. Autom. Sci. Eng. 12 (4), 1380–1395. doi:10.1109/TASE.2014.2336874.
Lebeau, P., Macharis, C., Van Mierlo, J., 2019. How to improve the total cost of ownership of electric vehicles: an analysis of the light commercial vehicle segment. World Electr. Veh. J. 10 (4), 90. doi:10.3390/wevj10040090.
Lei, C., Jiang, Z., Ouyang, Y., 2019. A discrete-continuous hybrid approach to periodic routing of waste collection vehicles with recycling operations. IEEE Trans. Intell. Transp. Syst. 1–10. doi:10.1109/TITS.2019.2951571.
Lei, C., Ouyang, Y., 2018. Continuous approximation for demand balancing in solving large-scale one-commodity pickup and delivery problems. Transp. Res. Part B 109, 90–109. doi:10.1016/j.trb.2018.01.009.
Li, X., Ma, J., Cui, J., Ghiasi, A., Zhou, F., 2016. Design framework of large-scale one-way electric vehicle sharing systems: a continuum approximation model. Transp. Res. Part B 88, 21–45. doi:10.1016/j.trb.2016.01.014.
Liu, M., Xu, X., 2018. Dockless bike-sharing reallocation based on data analysis: solving complex problem with simple method. In: 2018 IEEE Third International Conference on Data Science in Cyberspace (DSC). IEEE, Guangzhou, pp. 445–450. doi:10.1109/DSC.2018.00072.
Liu, Y., Szeto, W., Ho, S.C., 2018. A static free-floating bike repositioning problem with multiple heterogeneous vehicles, multiple depots, and multiple visits. Transp. Res. Part C 92, 208–242. doi:10.1016/j.trc.2018.02.008.
Masoud, M., Elhenawy, M., Almannaa, M.H., Liu, S.Q., Glaser, S., Rakotonirainy, A., 2019. Optimal assignment of e-scooter to chargers. In: 2019 IEEE Intelligent Transportation Systems Conference (ITSC). IEEE, Auckland, New Zealand, pp. 4204–4209. doi:10.1109/ITSC.2019.8917255.
Max Shen, Z.-J., Qi, L., 2007. Incorporating inventory and routing costs in strategic location models. Eur. J. Oper. Res. 179 (2), 372–389. doi:10.1016/j.ejor.2006.03.032.
McKenzie, G., 2019. Spatiotemporal comparative analysis of scooter-share and bike-share usage patterns in Washington, D.C.. J. Transp. Geogr. 78, 19–28. doi:10.1016/j.jtrangeo.2019.05.007.
Montoya, A., Guéret, C., Mendoza, J.E., Villegas, J.G., 2017. The electric vehicle routing problem with nonlinear charging function. Transp. Res. Part B 103, 87–110. doi:10.1016/j.trb.2017.02.004.
National Association of City Transportation Officials, 2018. Shared Micromobility in the U.S.: 2018. https://nacto.org/shared-micromobility-2018/.
National Association of City Transportation Officials, 2019. Shared Micromobility in the U.S.: 2019. https://nacto.org/shared-micromobility-2019/.
Newell, G.F., Daganzo, C.F., 1986. Design of multiple-vehicle delivery tours—I a ring-radial network. Transp. Res. Part B 20 (5), 345–363. doi:10.1016/0191-2615(86)90008-1.
Newell, G.F., Daganzo, C.F., 1986. Design of multiple vehicle delivery tours—II other metrics. Transp. Res. Part B 20 (5), 365–376. doi:10.1016/0191-2615(86)90009-3.
Ouyang, Y., 2007. Design of vehicle routing zones for large-scale distribution systems. Transp. Res. Part B 41 (10), 1079–1093. doi:10.1016/j.trb.2007.04.010.
Pal, A., Zhang, Y., 2017. Free-floating bike sharing: solving real-life large-scale static rebalancing problems. Transp. Res. Part C 80, 92–116. doi:10.1016/j.trc.2017.03.016.
Parragh, S.N., Doerner, K.F., Hartl, R.F., 2008. A survey on pickup and delivery problems: part II: transportation between pickup and delivery locations. J. Betriebswirtschaft 58 (2), 81–117. doi:10.1007/s11301-008-0036-4.
Pedregosa, F., Varoquaux, G., Gramfort, A., Michel, V., Thirion, B., Grisel, O., Blondel, M., Prettenhofer, P., Weiss, R., Dubourg, V., Vanderplas, J., Passos, A., Cournapeau, D., Brucher, M., Perrot, M., Duchesnay, E., 2011. Scikit-learn: machine learning in python. J. Mach. Learn. Res. 12, 2825–2830.
Pender, J., Tao, S., Wikum, A., 2020. A stochastic model for electric scooter systems. SSRN Electron. J. doi:10.2139/ssrn.3582320.
Raviv, T., Kolka, O., 2013. Optimal inventory management of a bike-sharing station. IIE Trans. 45 (10), 1077–1093. doi:10.1080/0740817X.2013.770186.
Raviv, T., Tzur, M., Forma, I.A., 2013. Static repositioning in a bike-sharing system: models and solution approaches. EURO J. Transp. Logist. 2 (3), 187–229. doi:10.1007/s13676-012-0017-6.
Regue, R., Recker, W., 2014. Proactive vehicle routing with inferred demand to solve the bikesharing rebalancing problem. Transp. Res. Part E 72, 192–209. doi:10.1016/j.tre.2014.10.005.
Reiss, S., Bogenberger, K., 2015. GPS-data analysis of Munich's free-floating bike sharing system and application of an operator-based relocation strategy. In: 2015 IEEE 18th International Conference on Intelligent Transportation Systems. IEEE, Gran Canaria, Spain, pp. 584–589. doi:10.1109/ITSC.2015.102.
Reiss, S., Bogenberger, K., 2016. Validation of a relocation strategy for Munich's bike sharing system. Transp. Res. Procedia 19, 341–349. doi:10.1016/j.trpro.2016.12.093.
Sayarshad, H., Tavassoli, S., Zhao, F., 2012. A multi-periodic optimization formulation for bike planning and bike utilization. Appl. Math. Model. 36 (10), 4944–4951. doi:10.1016/j.apm.2011.12.032.
Schuijbroek, J., Hampshire, R., van Hoeve, W.-J., 2017. Inventory rebalancing and vehicle routing in bike sharing systems. Eur. J. Oper. Res. 257 (3), 992–1004. doi:10.1016/j.ejor.2016.08.029.
Smith, M., Castellano, J., 2015. Costs Associated With Non-Residential Electric Vehicle Supply Equipment - Factors to Consider in the Implementation of Electric Vehicle Charging Stations. Technical Report. U.S. Department of Energy Vehicle Technologies Office.
Soriguera, F., Jiménez-Meroño, E., 2020. A continuous approximation model for the optimal design of public bike-sharing systems. Sustain. Cities Soc. 52, 101826. doi:10.1016/j.scs.2019.101826.
StoreDot, 2020. StoreDot: Ultra-fast charging batteries for EVs & more. https://www.store-dot.com.
Swift, B., 2019. Seattle's Bike Share Comparison. https://www.bikeswift.com/blogs/bike-swift-blog/seattles-bike-share-comparison.
Team, T., 2018. What Drives Value At Electric Scooter Sharing Startups Like Bird?https://www.forbes.com/sites/greatspeculations/2018/05/01/what-drives-value-at-electric-scooter-sharing-startups-like-bird/.
Toll, M., 2018. Love Lime but want your own electric scooter? Here are your best options. https://electrek.co/2018/10/26/buying-an-electric-scooter/.
Toll, M., 2019. Hyundai electric scooter unveiled that mounts to and charges in your car. https://electrek.co/2019/08/28/hyundai-unveils-electric-scooter-mounts-car-charging/.
Usama, M., Shen, Y., Zahoor, O., 2019. Towards an energy efficient solution for bike-sharing rebalancing problems: a battery electric vehicle scenario. Energies 12 (13), 2503. doi:10.3390/en12132503.
Xu, M., Meng, Q., Liu, Z., 2018. Electric vehicle fleet size and trip pricing for one-way carsharing services considering vehicle relocation and personnel assignment. Transp. Res. Part B 111, 60–82. doi:10.1016/j.trb.2018.03.001.
Zhang, D., Yu, C., Desai, J., Lau, H., Srivathsan, S., 2017. A time-space network flow approach to dynamic repositioning in bicycle sharing systems. Transp. Res. Part B 103, 188–207. doi:10.1016/j.trb.2016.12.006.